PLOS ONE

The nhppp package for simulating non-homogeneous Poisson point processes in R.

--Manuscript Draft--

Manuscript Number:	PONE-D-24-07749R2
Article Type:	Research Article
Full Title:	The nhppp package for simulating non-homogeneous Poisson point processes in R.
Short Title:	Simulating NHPPPs
Corresponding Author:	Thomas Trikalinos, MD PhD Brown University School of Public Health Providence, UNITED STATES OF AMERICA
Keywords:	stochastic point processes; counting processes; discrete event simulation; time-to-event simulation; R
Abstract:	We introduce the nhppp package for simulating events from one dimensional non-homogeneous Poisson point processes (NHPPPs) in R fast and with a small memory footprint. We developed it to facilitate the sampling of event times in discrete event and statistical simulations. The package's functions are based on three algorithms that provably sample from a target NHPPP: the time-transformation of a homogeneous Poisson process (of intensity one) via the inverse of the integrated intensity function; the generation of a Poisson number of order statistics from a fixed density function; and the thinning of a majorizing NHPPP via an acceptance-rejection scheme. We present a study of numerical accuracy and time performance of the algorithms. We illustrate use with simple reproducible examples.
Order of Authors:	Thomas Trikalinos, MD PhD
	Yuliia Sereda
Opposed Reviewers:	
Response to Reviewers:	Please see the uploaded pdf "response_to_reviewers.pdf"
Additional Information:	
Question	**Response**
Financial Disclosure Enter a financial disclosure statement that describes the sources of funding for the work included in this submission. Review the submission guidelines for detailed requirements. View published research articles from *PLOS ONE* for specific examples. This statement is required for submission and **will appear in the published article** if the submission is accepted. Please make sure it is accurate.	Yes

Powered by Editorial Manager® and ProduXion Manager® from Aries Systems Corporation

Funded studies Enter a statement with the following details: • Initials of the authors who received each award • Grant numbers awarded to each author • The full name of each funder • URL of each funder website • Did the sponsors or funders play any role in the study design, data collection and analysis, decision to publish, or preparation of the manuscript? Did you receive funding for this work?	
Please add funding details. as follow-up to "**Financial Disclosure** Enter a financial disclosure statement that describes the sources of funding for the work included in this submission. Review the submission guidelines for detailed requirements. View published research articles from *PLOS ONE* for specific examples. This statement is required for submission and **will appear in the published article** if the submission is accepted. Please make sure it is accurate. **Funded studies** Enter a statement with the following details: • Initials of the authors who received each award • Grant numbers awarded to each author • The full name of each funder • URL of each funder website • Did the sponsors or funders play any role in the study design, data collection and analysis, decision to publish, or preparation of the manuscript? Did you receive funding for this work?"	TAT and YS were funded from grant U01CA265750 from the National Cancer Institute (https://www.cancer.gov). The funder played no role in the study design, analysis, decision to publish, or the preparation of the manuscript.
Please select the country of your main research funder (please select carefully as in some cases this is used in fee calculation).	UNITED STATES - US

as follow-up to "**Financial Disclosure** Enter a financial disclosure statement that describes the sources of funding for the work included in this submission. Review the submission guidelines for detailed requirements. View published research articles from *PLOS ONE* for specific examples. This statement is required for submission and **will appear in the published article** if the submission is accepted. Please make sure it is accurate. **Funded studies** Enter a statement with the following details: • Initials of the authors who received each award • Grant numbers awarded to each author • The full name of each funder • URL of each funder website • Did the sponsors or funders play any role in the study design, data collection and analysis, decision to publish, or preparation of the manuscript? Did you receive funding for this work?"	
Competing Interests Use the instructions below to enter a competing interest statement for this submission. On behalf of all authors, disclose any competing interests that could be perceived to bias this work—acknowledging all financial support and any other relevant financial or non-financial competing interests. This statement is required for submission and **will appear in the published article** if the submission is accepted. Please make sure it is accurate and that any funding sources listed in your Funding Information later in the submission form are also declared in your Financial Disclosure statement.	The authors have declared that no competing interests exist.

View published research articles from *PLOS ONE* for specific examples. **NO authors have competing interests** Enter: *The authors have declared that no competing interests exist.* **Authors with competing interests** Enter competing interest details beginning with this statement: *I have read the journal's policy and the authors of this manuscript have the following competing interests: [insert competing interests here]* * typeset	
Ethics Statement Enter an ethics statement for this submission. This statement is required if the study involved: • Human participants • Human specimens or tissue • Vertebrate animals or cephalopods • Vertebrate embryos or tissues • Field research Write "N/A" if the submission does not require an ethics statement. General guidance is provided below. Consult the submission guidelines for detailed instructions. **Make sure that all information entered here is included in the Methods section of the manuscript.**	N/A

Format for specific study types **Human Subject Research (involving human participants and/or tissue)** • Give the name of the institutional review board or ethics committee that approved the study • Include the approval number and/or a statement indicating approval of this research • Indicate the form of consent obtained (written/oral) or the reason that consent was not obtained (e.g. the data were analyzed anonymously) **Animal Research (involving vertebrate animals, embryos or tissues)** • Provide the name of the Institutional Animal Care and Use Committee (IACUC) or other relevant ethics board that reviewed the study protocol, and indicate whether they approved this research or granted a formal waiver of ethical approval • Include an approval number if one was obtained • If the study involved *non-human primates*, add *additional details* about animal welfare and steps taken to ameliorate suffering • If anesthesia, euthanasia, or any kind of animal sacrifice is part of the study, include briefly which substances and/or methods were applied **Field Research** Include the following details if this study involves the collection of plant, animal, or other materials from a natural setting: • Field permit number • Name of the institution or relevant body that granted permission	
Data Availability Authors are required to make all data underlying the findings described fully available, without restriction, and from the time of publication. PLOS allows rare exceptions to address legal and ethical concerns. See the PLOS Data Policy and FAQ for detailed information.	Yes - all data are fully available without restriction

Powered by Editorial Manager® and ProduXion Manager® from Aries Systems Corporation

A Data Availability Statement describing where the data can be found is required at submission. Your answers to this question constitute the Data Availability Statement and **will be published in the article**, if accepted. **Important:** Stating 'data available on request from the author' is not sufficient. If your data are only available upon request, select 'No' for the first question and explain your exceptional situation in the text box. Do the authors confirm that all data underlying the findings described in their manuscript are fully available without restriction?	
Describe where the data may be found in full sentences. If you are copying our sample text, replace any instances of XXX with the appropriate details. • If the data are **held or will be held in a public repository**, include URLs, accession numbers or DOIs. If this information will only be available after acceptance, indicate this by ticking the box below. For example: *All XXX files are available from the XXX database (accession number(s) XXX, XXX.*). • If the data are all contained **within the manuscript and/or Supporting Information files**, enter the following: *All relevant data are within the manuscript and its Supporting Information files.* • If neither of these applies but you are able to provide **details of access elsewhere**, with or without limitations, please do so. For example: *Data cannot be shared publicly because of [XXX]. Data are available from the XXX Institutional Data Access / Ethics Committee (contact via XXX) for researchers who meet the criteria for access to confidential data.* *The data underlying the results presented in the study are available from (include the name of the third party*	There are no data associated with the manuscript. All the code to generate the exhibits is provided as supplementary information.

and contact information or URL). • This text is appropriate if the data are owned by a third party and authors do not have permission to share the data. * typeset	
Additional data availability information:	Tick here if the URLs/accession numbers/DOIs will be available only after acceptance of the manuscript for publication so that we can ensure their inclusion before publication.

15 July, 2024

Dear Editor,

We are submitting our second revision of our paper *"The* **nhppp** *package for simulating non-homogeneous Poisson point processes in* `R`*"* for your consideration for publication in *PLOS ONE*.

Per instructions, we have uploaded a tracked-changes version of the manuscript, where additions are in red font.

We have made edits to the manuscript to reply to the comments from this peer review round. Point to point replies to comments are listed in the Response Letter (uploaded separately). For this second round of the peer-review process, I observe that:

1. I have not received any clarifications on my questions about the Editors' comments from the first round of revisions. I, therefore, deduce that the Editor's comments from the first review round were due to a logistical mix up with another paper.

2. In the first review round, I asked the Editor and Reviewer 2 for clarifications on the comments by Reviewer 2, which were terse, unclear, nonspecific, and vague. I have received no replies. This impresses me as highly irregular. I claim that Reviewer 2 did not discharge his or her academic responsibilities satisfactorily in the first and second rounds of peer review. This Reviewer's lapses hinder me in discharging my own responsibilities as an author.

3. Reviewers 4 and 6 observe that the paper would also be appropriate for the `R` *Journal*. We opted to submit to *PLOS ONE* because our paper also includes a review of some theory and a numerical study. I believe that *PLOS ONE* is an appropriate place for the paper. Reviewer 6 also observes that *PLOS ONE* has published papers on *R packages*, which is accurate: I find at least 86 publications introducing `R` packages in *PLOS ONE*.[1]

4. Reviewer 5 recommends that we *"supplement the conclusion with quantitative results, particularly highlighting the advantages of their package over existing toolboxes, such as improvements in efficiency and accuracy, among other metrics."*

   Extensive quantitative analyses are presented in Sections 6 and 7 of the manuscript, and in Figures 2 through 7 and Tables 3 through 8. These sections include a detailed comparisons with all packages that include the ability to simulate from NHPPPs, and document that some of the packages simulate only approximately. Please advise.

Because of these observations, I ask that the complete peer review record for this submission be made publicly available to the fullest extent allowed by the Journal.

As described in the manuscript, a preprint of this work was submitted to `arXiv`,[2] the package

[1] Based on the PubMed query `PLOS ONE[so] AND "R package"[ti]` on July 15, 2024.

[2] The preprint is uploaded as a 'Related Manuscript', per submission instructions

is on the Comprehensive R Archive Network, and its code is in a publicly accessible GitHub repository.

No part of this manuscript is considered for peer review and publication elsewhere.

We hope that the six reviewers and you will deem the manuscript worthy of publication.

Regards,

TA Trikalinos

Manuscript
Click here to access/download;Manuscript;nhppp_package_PLOSONE_R2-

The **nhppp** package for simulating non-homogeneous Poisson point processes in R

Thomas A. Trikalinos[1,2,3,*], Yuliia Sereda[1]

1 Center for Evidence Synthesis in Health, Brown University, Providence, RI, USA

2 Department of Health Services, Policy & Practice, Brown University, Providence, RI, USA

3 Department of Biostatistics, Brown University, Providence, RI, USA

* thomas_trikalinos@brown.edu

Abstract

We introduce the **nhppp** package for simulating events from one dimensional non-homogeneous Poisson point processes (NHPPPs) in R fast and with a small memory footprint. We developed it to facilitate the sampling of event times in discrete event and statistical simulations. The package's functions are based on three algorithms that provably sample from a target NHPPP: the time-transformation of a homogeneous Poisson process (of intensity one) via the inverse of the integrated intensity function; the generation of a Poisson number of order statistics from a fixed density function; and the thinning of a majorizing NHPPP via an acceptance-rejection scheme. We present a study of numerical accuracy and time performance of the algorithms. We illustrate use with simple reproducible examples.

1 Introduction

It is often desirable to simulate series of events (stochastic point processes) so that the intensity of their occurrence varies over time. Examples include events such as the occurrence of death and occurrences of symptoms, infections, or tumors over a person's lifetime. The non-homogeneous Poisson point process (NHPPP), which generalizes the simpler homogeneous-Poisson, Weibull, and Gompertz point processes, is a widely used model for such series of events. NHPPPs can model complicated event patterns given a suitable intensity function. They are, therefore, useful in statistical and mathematical model simulation.

An NHPPP has the properties that the number of events in all non-overlapping time intervals are independent random variables and that, within each time interval, the number of events is Poisson distributed. Thus an NHPPP is a memoryless point process. A large number of phenomena may reasonably conform with these properties.

NHPPPs have been used in the simulation analysis of queues in queuing theory and operations research [1, 2]; hospital operations [3]; ambulance services [4, 5]; traffic accidents [6]; product and network reliability [7]; and the modeling of cancer [8–11], heart disease [12], and dementia [13, 14], among other applications [15]. NHPPPs are used so widely in part because their assumptions are often plausible. For example, when modeling traffic accidents along a road, it may be plausible to assume that individual accidents are independent of each other, but they happen in some locations more often because the probability of an accident depends on local aspects of the road, such as turns, slopes, and propensity for slippery conditions. Similarly, when modeling the impact of screening strategies on colorectal cancer outcomes at the population level, it is probably plausible to assume that, for each person, the emergence of precancerous lesions (adenomas) over a time interval is independent of whether such lesions emerged in other non-overlapping time intervals. In these examples, the intensity of event occurrence over the carrier space (the probability of a traffic accident along a road; and the probability that an adenoma will emerge in a person's colon at different ages) is captured by the NHPPP's intensity function. An NHPPP can model complicated event patterns using intensity functions that vary over the carrier space (e.g., length of road, time).

The **nhppp** package in `R` contains functions for the simulation of NHPPPs over a one-dimensional carrier space, which we will take to represent time [16, 17]. Table 1 summarizes the functions implemented in **nhppp** as of version 0.1.4. You can install the development version of **nhppp** with

```
R> # install.packages("devtools")
R> devtools::install_github("bladder-ca/nhppp")
```

or the release version with

```
R> install.packages("nhppp")
```

We review NHPPPs in Section 2 and algorithms for sampling from constant rate Poisson point processes in Section 3. We introduce the three sampling algorithms that are implemented in the package in Section 4. We discuss special functional forms for the intensity function (constant, piecewise constant, linear, and log-linear) in Section 5. We describe **nhppp** versus other `R` packages that can simulate from one dimensional NHPPPs in Section 6 and present a numerical study in Section 7. We summarize in Section 8.

2 The Poisson point process

2.1 Definition

The Poisson point process is a stochastic series of events on the real line. For some sequence of events, let $N(t, t+\Delta t)$ be the number of events in the interval $(t, t+\Delta t]$. If for some positive intensity λ and, as $\Delta t \to 0$,

$$\begin{aligned} \Pr[N(t,t+\Delta t)=0] &= 1-\lambda\Delta t + o(\Delta t), \\ \Pr[N(t,t+\Delta t)=1] &= \lambda\Delta t + o(\Delta t), \\ \Pr[N(t,t+\Delta t)>1] &= o(\Delta t), \text{ and} \\ N(t,t+\Delta t) &\perp\!\!\!\perp N(0,t), \end{aligned} \tag{1}$$

then that sequence of events is a Poisson point process. In Equation (1), the third statement demands that events occur one at a time. The fourth statement implies that

Table 1. Functions in nhppp.

Intensity function	Function name	Function simulates...
Constant	`ppp_n()`	exactly n events in $[a, b)$
	`ppp_next_n()`	the next n events in $[a, \infty)$
	`ppp_sequential()`, `ppp_orderstat()`	≥ 0 events in $[a, b)$
	`ztppp()`	≥ 1 events in $[a, b)$
Time-varying, special cases, non-vectorized	`draw_sc_linear()`	≥ 0 events in $[a, b)$ from $\lambda(t) = \alpha + \beta t$
	`draw_sc_loglinear()`	≥ 0 events in $[a, b)$ from $\lambda(t) = \exp(\alpha + \beta t)$
	`draw_sc_step()`	≥ 0 events in $[a, b)$ from piecewise constant $\lambda(t)$ with uneven intervals
	`draw_sc_step_regular()`	≥ 0 events in $[a, b)$ from piecewise constant $\lambda(t)$ with regular intervals
	`ztdraw_sc_linear()`	≥ 1 events in $[a, b)$ from $\lambda(t) = \alpha + \beta t$
	`ztdraw_sc_loglinear()`	≥ 1 events in $[a, b)$ from $\lambda(t) = \exp(\alpha + \beta t)$
Time varying, special cases, vectorized	`vdraw_sc_step_regular()`	≥ 0 events in $[a, b)$ from piecewise constant $\lambda(t)$ with regular intervals
	`vztdraw_sc_step_regular()`	≥ 1 events in $[a, b)$ from piecewise constant $\lambda(t)$ with regular intervals
Time-varying, general case, non-vectorized	`draw()`	(wrapper function)
	`draw_cumulative_intensity_inversion()`	≥ 0 events in $[a, b)$ from $\Lambda(t), \Lambda^{-1}(t)$
	`draw_cumulative_intensity_orderstats()`	≥ 0 events in $[a, b)$ from $\Lambda(t), \Lambda^{-1}(t)$
	`draw_intensity()`	≥ 0 events in $[a, b)$ from $\lambda(t), \lambda_*(t)$
	`draw_intensity_step()`	≥ 0 events in $[a, b)$ from $\lambda(t)$ and piecewise constant $\lambda_*(t)$
	`ztdraw_cumulative_intensity()`	≥ 1 events in $[a, b)$ from $\Lambda(t), \Lambda^{-1}(t)$
	`ztdraw_intensity()`	≥ 1 events in $[a, b)$ from $\lambda(t), \lambda_*(t)$
	`ztdraw_intensity_step()`	≥ 1 events in $[a, b)$ from $\lambda(t)$ and piecewise constant $\lambda_*(t)$
Time varying, general case, vectorized	`vdraw()`	(wrapper function)
	`vdraw_intensity_step_regular()`	≥ 0 events in $[a, b)$ from $\lambda(t)$ and piecewise constant $\lambda_*(t)$
	`vztdraw_intensity_step_regular()`	≥ 1 events in $[a, b)$ from $\lambda(t)$ and piecewise constant $\lambda_*(t)$
(Helper function)	`get_step_majorizer()`	(obtains piecewise constant $\lambda_*(t)$ from $\lambda(t)$)

The table pertains to version 0.1.4 of **nhppp**. $\lambda(t)$ is an intensity function, $\lambda_*(t)$ a majorizer function for $\lambda(t)$, $\Lambda(t)$ the integrated intensity function, and $\Lambda^{-1}(t)$ the inverse function (preimage) of $\Lambda(t)$.

the process is memoryless: For any time t_0, the behavior of the process is independent to what happened before that time.

2.2 Homogeneous Poisson point process and counting process

Assume that the next event after time t_0 happens at time $t_0 + X$. It follows from the above definition (see [18, par. 4.1]) that, for a constant λ, X is exponentially distributed

$$X \sim \text{Exponential}(\lambda), \tag{2}$$

and that the number of events is Poisson distributed over the compact interval $(a, b]$, i.e.,

$$N(a, b) \sim \text{Poisson}(\lambda(b - a)). \tag{3}$$

Equation (2) generates the homogeneous Poisson point process $Z_1 = t_0 + X_1, Z_2 = Z_1 + X_2, \ldots$, where Z_i is the time of arrival of event i and X_i the inter-arrival times. We will use $Z_{(j)}$ to denote the event in position j when events are ordered in increasing time. Equation (3) describes the corresponding (dual) counting process $N_1 = N(t_0, Z_1), N_2 = N(t_0, Z_2), \ldots$, where N_i is the total number of events from time t_0 to time Z_i. The point process (the sequence $[Z_i]$ of event times) and the counting process (the sequence $[N_i]$ of cumulants) are two sides of the same coin.

Sampling from the constant rate point process in (2) is discussed in Section 3.

2.3 Non homogeneous Poisson point process and counting process

When the intensity function changes over time, the homogeneous Poisson point process generalizes to its non-stationary counterpart, an NHPPP, with intensity function $\lambda(t) > 0$. For details see reference [18, par 4.2]. Then, the number of events over the interval $(a, b]$ becomes

$$N(a, b) \sim \text{Poisson}(\Lambda(a, b)), \tag{4}$$

where $\Lambda(a, b) = \int_a^b \lambda(t)\, dt$ is the integrated intensity or cumulative intensity of the NHPPP. Equation (4) describes the counting process of the NHPPP, which in turn implies a stochastic point process – a distribution of events over time.

Here the simulation task is to sample event times from the point process that corresponds to intensity function $\lambda(t)$, or equivalently, to the integrated intensity

function $\Lambda(t) = \int_0^t \lambda(s)\ ds$ (Section 4). (With some abuse of notation, we define $\Lambda(t) \coloneqq \Lambda(0, t)$ when $a = 0$.)

2.3.1 A note on zero intensity processes

In (1), λ is strictly positive but in **nhppp** we allow it to be non-negative. If $\lambda = 0$, $\Pr[N(t, t + \Delta t) = 0] = 1$ and $\Pr[N(t, t + \Delta t) \geq 1] = 0$. This means that no events occur and the stochastic point process in the interval $(t, t + \Delta t]$ is denegerate. Allowing $\lambda(t) \geq 0$ has no bearing on the results of simulations. If

$$\lambda(t) \begin{cases} > 0, \text{ for } t \in (a, b] \\ = 0, \text{ for } t \in (b, c] \\ > 0, \text{ for } t \in (c, d] \end{cases}$$

we can always ignore the middle interval in which no events happen.

2.4 Properties that are important for simulation

2.4.1 Composability and decomposability of NHPPPs

The definition (1) implies that NHPPPs are composable [18, par. 4.2]: merging two NHPPPs with intensity functions $\lambda_1(t), \lambda_2(t)$ yields a new NHPPP with intensity function $\lambda(t) = \lambda_1(t) + \lambda_2(t)$. The reciprocal is also true: one can decompose an NHPPP with intensity function $\lambda(t)$ into two NHPPPs, one with intensity function $\lambda_1(t) < \lambda(t)$ and one with intensity function $\lambda_2(t) = \lambda(t) - \lambda_1(t)$. An induction argument extends the above to merging and decomposing three or more processes.

The composability and decomposability properties are important for simulation because they

- give the flexibility to simulate several parallel NHPPPs independently versus to merge them, simulate from the merged process, and then attribute the realized events to the component processes by assigning the i-th event to the j-th process with probability $\lambda_j(Z_i)/\lambda(Z_i)$, where $\lambda(t) = \sum \lambda_j(t)$.
- motivate a general sampling algorithm (Algorithm 4, "thinning" [19]) that simulates a target NHPPP with intensity $\lambda_1(t)$ by first drawing events from an

easy-to-sample NHPPP with intensity $\lambda(t) > \lambda_1(t)$, and then accepts sample i with probability $\lambda_1(Z_i)/\lambda(Z_i)$.

2.4.2 Transformations of the time axis

Strictly monotonic transformations of the carrier space of an NHPPP yield an NHPPP [20]. Consider an NHPPP with intensity functions $\lambda(t)$ and a strictly monotonic transformation of the time axis $u : t \mapsto \tau$ that is differentiable once almost everywhere. On the transformed time axis the point process is an NHPPP with intensity function

$$\rho(\tau) = \lambda(\tau) \left(\frac{du}{dt} \right)^{-1}. \tag{5}$$

This property is important for simulation because

- it motivates the use of another general sampling algorithm (Algorithm 5, "time transformation" or "inversion", [20]): A smart choice for u yields an easy to sample point process. The event times in the original time scale can be obtained as $Z_i = u^{-1}(\zeta_i)$, where ζ_i is the i-th event in the transformed time axis and u^{-1} is the inverse function of u.
- given that at least i events have realized in the time interval $(a, b]$, it makes it possible to draw events $Z_{(j)}, j < i$ given event $Z_{(i)}$. This is useful for simulating earlier events conditional on the occurrence of a subsequent event. Choosing $u(t) := Z_{(i)} - t$ makes the time count backwards from $Z_{(i)}$. In this reversed clock we draw as if in forward time exactly $i - 1$ events $\zeta_{(1)}, \zeta_{(2)}, \ldots, \zeta_{(i-1)}$. Back transforming yields all preceding events.

Table 2 summarizes the common simulation tasks, such as simulating single events (at most one, exactly one), a series of events (possibly demanding the occurrence of at least one event), or the occurrence of a prior (event $i - 1$ given $Z_{(i)}$). The **nhppp** package implements functions to simulate these tasks for general $\lambda(t)$ or $\Lambda(t)$.

3 Sampling the constant rate Poisson process

Sampling the constant rate Poisson process is straightforward. Algorithms 1 and 2 are two ways to sample event times in interval $(a, b]$ with constant intensity λ. Algorithm 3

Table 2. Common simulation needs in discrete event simulation.

#	Sampling task	Sampled times	Number of sampled events	Example
I	Any next event	$\{\}$ or $\{Z_{(1)}\}$	0 or 1	Single event that may (or may not) occur in the interval: death, progression from Stage I to Stage II cancer.
II	Exactly one next event	$\{Z_{(1)}\}$	1	Single event which must occur in the interval: death from any cause in a lifetime-horizon simulation.
III	Any and all events	$\{\}$ or $\{Z_{(1)}, Z_{(2)}, \dots\}$	≥ 0	Zero, one, or more events: emergence of one or more bladder tumors.
IV	At least one next event	$\{Z_{(1)}, Z_{(2)}, \dots\}$	≥ 1	One or more events: emergence of bladder tumors when simulating only patients with bladder tumors.
V	Event $i-1$ given $Z_{(i)}$	$\{Z_{(i-1)}\}$	1	Find the previous event when simulating conditional on a future event: time of symptom onset given the time of symptom-driven diagnosis; onset of Stage I cancer given progression from Stage I to Stage II cancer.

All listed tasks involve sampling events over the interval $(a, b]$ with known $\lambda(t)$ or $\Lambda(t)$.

describes sampling event times conditional on observing at least k events within the interval of interest.

3.1 Sequential sampling

Algorithm 1 samples events sequentially, using the fact that the inter-event times X_i are exponentially distributed with mean λ^{-1} [18, par. 4.1]. It involves generation only of exponential random variates, which is cheap on modern hardware. To sample at most k events, change the condition for the while loop in line 3 to

$$\textbf{while } t < b \ \& \ |\mathcal{Z}| < k \textbf{ do}.$$

The package's `ppp_sequential()` function implements constant-rate sequential sampling that returns a vector with zero or more event times in the interval $[a, b)$. The `range_t` argument is a two-values vector with the bounds a, b. Setting the optional argument `atmost1` to `TRUE` from its default value of `FALSE` returns the first event or an empty vector, depending on whether at least one event is drawn in the interval.

Algorithm 1 Sequential sampling of events in interval $(a, b]$ with constant intensity λ.

Require: $t \in (a, b]$
$t \leftarrow a$
$\mathcal{Z} \leftarrow \emptyset$ ▷ $\mathcal{Z}$ is an ordered set
while $t < b$ **do** ▷ Up to k earliest points: **while** $t < b$ & $|\mathcal{Z}| < k$ **do**
  $X \leftarrow X \sim \text{Exponential}(\lambda^{-1})$ ▷ Mean-parameterized
  $t \leftarrow t + X$
  if $t < b$ **then**
    $\mathcal{Z} \leftarrow \mathcal{Z} \cup \{t\}$
  end if
end while
return $\mathcal{Z}$

```
R> library("nhppp")

R> ppp_sequential(range_t = c(7, 10), rate = 1, atmost1 = FALSE)

[1] 7.673885 8.650502 9.011229 9.407575
```

nhppp functions can accept a user provided random number stream object via the `rng_stream` option.

```
R> library("rstream")

R> S <- new("rstream.mrg32k3a")

R> ppp_sequential(range_t = c(7, 10), rate = 1, rng_stream = S)

[1] 8.793702
```

3.2 Sampling using order statistics

Algorithm 2 Sampling events in interval $(a, b]$ with constant intensity λ using order statistics.

Require: $t \in (a, b]$
$N \leftarrow N \sim \text{Poisson}\big(\lambda(b - a)\big)$
$t \leftarrow a$
$\mathcal{Z} \leftarrow \emptyset$ ▷ $\mathcal{Z}$ is an ordered set
if N > 0 **then**
  for $i \in [N]$ **do**:
    $U_i \leftarrow U_i \sim \text{Uniform}(0, 1)$ ▷ Generate order statistics
    $\mathcal{Z} \leftarrow \mathcal{Z} \cup \{a + (b - a)U_i\}$
  end for
  $\mathcal{Z} \leftarrow \text{sort}(\mathcal{Z})$
end if
return $\mathcal{Z}$ ▷ Up to k earliest points: **return** $\{Z_{(i)} \mid i \leq k\ , Z_{(i)} \in \mathcal{Z}\}$

Algorithm 2 first draws the number of events in $(a, b]$ from a Poisson distribution. Conditional on the number of events, the event times Z_i are uniformly distributed over $(a, b]$ [18, par. 4.1]. The algorithm returns the order statistics $[Z_{(i)}]$, obtained by sorting the event times $[Z_i]$ in ascending order. It is necessary to generate all event times to generate the order statistics. Thus, to sample at most k event times we should return the earliest k event times, and line 11 of the Algorithm would be changed to

$$\textbf{return } \{Z_{(i)} \mid i \leq k, Z_{(i)} \in \mathcal{Z}\}.$$

The `ppp_orderstat()` function implements constant-rate sampling via the order-statistics algorithm.

```
R> ppp_orderstat(range_t = c(3.14, 6.28), rate = 1/2)
```

```
[1] 3.141663 5.700931
```

3.3 Sampling conditional on observing at least m events

Algorithm 3 Sampling with constant intensity λ conditional that at least m events occurred in interval $(a, b]$. Relies on generating order statistics analogously to Algorithm 2.

Require: $t \in (a, b]$
1: $N \leftarrow N \sim \text{TruncatedPoisson}_{N \geq m}\big(\lambda(b-a)\big)$ ▷ $(m-1)$-truncated Poisson
2: $t \leftarrow a$
3: $\mathcal{Z} \leftarrow \emptyset$ ▷ $\mathcal{Z}$ is an ordered set
4: **if** N > 0 **then**
5: **for** $i \in [N]$ **do**:
6: $U_i \leftarrow U_i \sim \text{Uniform}(0, 1)$ ▷ Generate order statistics
7: $\mathcal{Z} \leftarrow \mathcal{Z} \cup \{a + (b-a)U_i\}$
8: **end for**
9: $\mathcal{Z} \leftarrow \text{sort}(\mathcal{Z})$
10: **end if**
11: **return** $\mathcal{Z}$ ▷ Up to k earliest points: **return** $\{Z_{(i)} \mid i \leq k\ , Z_{(i)} \in \mathcal{Z}\}$

Algorithm 3 is used to generate a point process conditional on observing at least m events. For example, if λ is the intensity of tumor generation, it can be used to simulate times of tumor emergence among patients with at least one ($m = 1$) tumor. To return the up to k earliest events, we modify line 11 the same way as for Algorithm 2. As an example, in a lifetime simulation we can sample the time of all-cause death by setting in Algorithm 3 $m = 1$, so that at least one event will happen in $(a, b]$, and $k = 1$, to sample only the time of the first event $Z_{(1)}$.

To sample exactly m events, change line 1 of Algorithm 3 to

$$N \leftarrow m.$$

Function `ztppp()` simulates times conditional on drawing at least one event - i.e., setting $m = 1$ in Algorithm 3 to sample from a zero truncated Poisson distribution in line 1.

```
R> ztppp(range_t = c(0, 10), rate = 0.001, atmost1 = FALSE)

[1] 4.411277
```

Function `ppp_n()` simulates times conditional on drawing exactly m events.

```
R> ppp_n(size = 4, range_t = c(0, 10))

[1] 1.762014 2.902897 6.751627 9.733794
```

4 The general sampling algorithms used in nhppp

The **nhppp** package uses three well known general sampling algorithms, namely thinning, time transformation or inversion, and order-statistics. These algorithms are efficiently combined to sample from special cases, including cases where the intensity function is a piecewise constant, linear, or log-linear function of time, as described in Section 5.2.

The thinning algorithm works with the intensity function $\lambda(t)$, which is commonly available. The inversion and order statistics algorithms have smaller computational cost than the thinning algorithm, but work with the integrated intensity function $\Lambda(t)$ and its inverse $\Lambda^{-1}(z)$, which may not be available. The generic function `draw()` is a wrapper function that dispatches to specialized functions depending on the provided arguments. It is useful for general tasks but the specialized functions are probably faster.

```
R> l <- function(t) t
R> L <- function(t) 0.5 * t^2
R> Li <- function(z) sqrt(2 * z)
R> draw(
+    lambda = l, lambda_maj = l(10), range_t = c(5, 10),
```

```
+    atmost1 = FALSE, atleast1 = FALSE
+  ) |> head(n = 5)

[1] 5.179473 5.374814 5.957391 5.992196 6.101935

R> draw(
+    Lambda = L, Lambda_inv = Li, range_t = c(5, 10),
+    atmost1 = FALSE, atleast1 = FALSE
+  ) |> head(n = 5)

[1] 5.219264 5.230747 5.369646 5.398531 5.618079
```

4.1 The thinning algorithm

The thinning algorithm relies on the decomposability of NHPPPs (Section 2.4) and is described in [19]. Let the target NHPPP have intensity function $\lambda(t)$ and $\lambda_*(t) \geq \lambda(t)$ for all $t \in (a, b]$ be a majorizing intensity function. Think of the majorizing function as an easy-to-sample function which is the sum of the intensity of the target point process $\lambda(t)$ and the intensity $\lambda_{reject}(t)$ of its complementary point-process,

$$\lambda_*(t) = \lambda(t) + \lambda_{reject}(t).$$

The acceptance-rejection scheme in Algorithm 4 generates proposal samples with intensity function $\lambda_*(t)$ and stochastically attributes them to the target process (to keep, with probability $\lambda(Z)/\lambda_*(Z)$) or its complement.

To sample the earliest k points, one can exit the for loop in lines 4-9 when k events have been sampled in line 7, or, alternatively, return the first up to k points in line 11.

A measure of the efficiency of Algorithm 4 is the proportion of samples that are accepted, which is

$$\frac{\int_a^b \lambda(t)\ \mathrm{d}t}{\int_a^b \lambda_*(t)\ \mathrm{d}t} \tag{6}$$

on average. Thus, the closer $\lambda_*(t)$ is to $\lambda(t)$, the more efficient the algorithm.

In practice, $\lambda_*(t)$ can be chosen as one of the special cases in Section 5, for which we have fast sampling algorithms. For example, it can be a piecewise constant majorizer. Algorithm A in S1 Appendix can automatically generate a piecewise constant majorizer

Algorithm 4 The thinning algorithm for sampling from $\lambda(t)$.

Require:

$\lambda_*(t) \geq \lambda(t)\ \forall\ t \in (a,])$ ▷ majorizing intensity function

$\mathcal{Z}_* = \{Z_i^* \mid Z_i^* \text{ are samples from } \lambda_*(t)\}$ ▷ $\mathcal{Z}_*$ is an ordered set

$N \leftarrow |\mathcal{Z}_*|$

$\mathcal{Z} \leftarrow \emptyset$ ▷ $\mathcal{Z}$ is an ordered set

if $N > 0$ **then**

  for $i \in [N]$ **do**:

    $U_i \leftarrow U_i \sim \text{Uniform}(0, 1)$

    if $U_i < \lambda(Z_{(i)}^*)/\lambda_*(Z_{(i)}^*)$ **then**

      $\mathcal{Z} \leftarrow \mathcal{Z} \cup \{Z_{(i)}^*\}$

    end if

  end for

end if

return $\mathcal{Z}$ ▷ Up to k earliest points: **return** $\{Z_{(i)} \mid i \leq k\ , Z_{(i)} \in \mathcal{Z}\}$

function for intensity functions that are monotonic and possibly non-continuous or Lipschitz continuous and possibly non-monotonic.

The **nhppp** package has functions that sample from time-varying intensity functions. The first function, `draw_intensity()`, expects a user-provided linear ($\lambda_*(t) = \alpha + \beta t$) or log-linear ($\lambda_*(t) = e^{\alpha+\beta t}$) majorizer function.

```
R> lambda_fun <- function(t) exp(0.02 * t)
R> draw_intensity(
+    lambda = lambda_fun, # linear majorizer
+    lambda_maj = c(intercept = 1.01, slope = 0.03),
+    exp_maj = FALSE, range_t = c(0, 10)
+  ) |> head (n = 5)

[1] 1.310245 2.094217 2.908682 3.268384 8.007606

R> draw_intensity(
+    lambda = lambda_fun, # log-linear majorizer
+    lambda_maj = c(intercept = 0.01, slope = 0.03),
+    exp_maj = TRUE, range_t = c(0, 10)
+  ) |> head (n = 5)

[1] 0.3406743 0.6079479 0.8441584 2.6424551 3.3185387
```

The second function, `draw_intensity_step()`, expects a user-provided piecewise

linear majorizer

$$\lambda_*(t) = \begin{cases} \lambda_1 & \text{for } t \in [a_1, b_1) = [a, b_1), \\ \dots & \\ \lambda_m & \text{for } t \in [a_m, b_m) \text{ with } a_m = b_{m-1}, \\ \dots & \\ \lambda_M & \text{for } t \in [a_M, b_M) = [a_M, b), \end{cases}$$

which is specified as a vector of length $M + 1$ including the points $(a, [b_m]_{m=1}^M)$ and a vector of length M with the values $[\lambda_m]_{m=1}^M$ in each subinterval of $(a, b]$. For example, the following code splits the interval $(0, 10]$ into $M = 10$ subintervals of length one. Because `lambda_fun()` is strictly increasing, its value at the upper bound of each subinterval is the supremum of the interval.

```
R> draw_intensity_step(
+    lambda = lambda_fun,
+    lambda_maj_vector = lambda_fun(1:10), # 1:10 (10 intensity values)
+    times_vector = 0:10 # 0:10 (11 interval bounds)
+  ) |> head(n = 5)
```

```
[1] 0.3825378 7.0822941 7.7839779 8.7766992 8.9554954
```

4.2 The time transformation or inversion algorithm

Algorithm 5 implements the time transformation or inversion algorithm from [20] and [18, par. 4.2]. As mentioned in Section 2.4, strictly monotonic transformations of the carrier space (here, time) of a Poisson point process yield another Poisson Point Process. In equation (5), choosing the transformation $\tau = u(t) = \Lambda(t)$, so that $\frac{du(t)}{dt} = \lambda(t)$, results in $\rho(\tau) = 1$.

This means (proof sketched in [18, par. 4.2]) that we can sample points from a Poisson point process with intensity one over the interval $(\tau_a, \tau_b] = (\Lambda(a), \Lambda(b)]$. Via a similar argument, we transform event times sampled on the transformed scale back to the original scale using $g(t) = \Lambda^{-1}(\tau)$. The transformations $u(\cdot), g(\cdot)$ are not unique – at least up to the group of affine transformations.

Function `draw_cumulative_intensity_inversion()` works with a cumulative intensity function $\Lambda(t)$ and its inverse $\Lambda^{-1}(z)$, if available. If the inverse function is not available (argument `Lambda_inv = NULL`), the Brent bisection algorithm is used to invert $\Lambda(t)$ numerically, at a performance cost [21].

```
R> Lambda_fun <- function(t) 50 * exp(0.02 * t) - 50
R> Lambda_inv_fun <- function(z) 50 * log((z + 50) / 50)
R> draw_cumulative_intensity_inversion(
+    Lambda = Lambda_fun,
+    Lambda_inv = Lambda_inv_fun,
+    range_t = c(5, 10.5),
+    range_L = Lambda_fun(c(5, 10.5))
+  ) |> head(n = 5)

[1]  6.458937  7.608496  9.060817  9.566278 10.076889
```

Algorithm 5 The time transformation or inversion algorithm for sampling given $\Lambda(t), \Lambda^{-1}(z)$ [18, 20]. The notation PoissonProcess_1 indicates sampling event times from a constant rate one Poisson point process.

Require: $\Lambda(t), \Lambda^{-1}(z), t \in (a, b]$ ▷ $\Lambda^{-1}(z)$ possibly numerically
1: $\tau_a \leftarrow \Lambda(a), \tau_b \leftarrow \Lambda(b)$
2: $\mathcal{C} \leftarrow \mathcal{C} \sim \text{PoissonProcess}_1(\tau_a, \tau_b)$ ▷ From Algorithm 1 (or 3 for conditional sampling)
3: $\mathcal{Z} \leftarrow \Lambda^{-1}(\mathcal{C})$ ▷ $\Lambda^{-1}(\cdot)$ as set function, meant elementwise
4: **return** $\mathcal{Z}$

4.3 The order statistics algorithm

The general order statistics algorithm (Algorithm 6) is a direct generalization of Algorithm 2. It first draws the number N of realized events. Conditional on N

$$\begin{aligned} U_{(i)} &= \frac{\Lambda(Z_{(i)}) - \Lambda(a)}{\Lambda(b) - \Lambda(a)} \sim \text{Uniform}(0, 1), \\ Z_{(i)} &= \Lambda^{-1}\Big(\Lambda(a) + U_{(i)}\big(\Lambda(b) - \Lambda(a)\big)\Big), \end{aligned} \tag{7}$$

as discussed in [19]. Algorithm 6 makes the above explicit.

Sampling up to k earliest points means returning the up to k earliest event times. If $\Lambda(t)$ is a positive linear function of time, λ is constant and Algorithm 6 becomes Algorithm 2.

Algorithm 6 The order statistics algorithm for sampling from an NHPPP given $\Lambda(t), \Lambda^{-1}(z)$.

Require: $\Lambda(t), \Lambda^{-1}(z), t \in (a, b]$ ▷ $\Lambda^{-1}(z)$ possibly numerically
$N \leftarrow N \sim \text{Poisson}\big(\Lambda(b) - \Lambda(a)\big)$
$t \leftarrow a$
$\mathcal{Z} \leftarrow \emptyset$ ▷ $\mathcal{Z}$ is an ordered set
if N > 0 **then**
  for $i \in [N]$ **do**:
    $U_i \leftarrow U_i \sim \text{Uniform}(0, 1)$ ▷ Generate order statistics
    $\mathcal{Z} \leftarrow \mathcal{Z} \cup \{\Lambda^{-1}\Big(\Lambda(a) + U_i\big(\Lambda(b) - \Lambda(a)\big)\Big)\}$
  end for
  $\mathcal{Z} \leftarrow \text{sort}(\mathcal{Z})$
end if
return $\mathcal{Z}$ ▷ Up to k earliest points: **return** $\{Z_{(i)} \mid i \leq k\ , Z_{(i)} \in \mathcal{Z}\}$

To sample conditional on observing at least m events in the interval $(a, b]$ see Algorithm B in S2 Appendix.

$$N \leftarrow N \sim \text{TruncatedPoisson}_{N \geq m}\big(\Lambda(b) - \Lambda(a)\big).$$

Function `draw_cumulative_intensity_orderstats()` works with a cumulative intensity function $\Lambda(t)$ and its inverse $\Lambda^{-1}(z)$, if available. Function `ztdraw_cumulative_intensity()` conditions that at least one event is sampled in the interval. As above, if the inverse function is not available (argument `Lambda_inv = NULL`), the Brent bisection algorithm is used to invert $\Lambda(t)$ numerically, at a performance cost.

```
R> draw_cumulative_intensity_orderstats(
+    Lambda = Lambda_fun,
+    Lambda_inv = Lambda_inv_fun,
+    range_t = c(4.1, 7.6)
+  )

[1] 5.091581 5.526070 5.601576 5.762498 6.495684

R> ztdraw_cumulative_intensity(
+    Lambda = Lambda_fun,
+    Lambda_inv = Lambda_inv_fun,
+    range_t = c(4.1, 7.6)
+  )
```

```
[1] 5.063676 6.682454 6.749162 6.926164 7.298342
```

5 Special cases

The **nhppp** package implements several special cases where the intensity function $\lambda(\cdot)$, the integrated intensity function $\Lambda(\cdot)$, and its inverse $\Lambda^{-1}(\cdot)$ have straightforward analytical expressions.

5.1 Sampling a piecewise constant NHPPP

Functions `draw_sc_step()` and `draw_sc_step_regular()` sample piecewise constant intensity functions based on Algorithm 5. The first can work with unequal-length subintervals $(a_m, b_m]$. The second results in a small computational time improvement when all subintervals are of equal length.

```
R> draw_sc_step(
+    lambda_vector = 1:5, times_vector = c(0.5, 1, 2.4, 3.1, 4.9, 5.9),
+    atmost1 = FALSE, atleast1 = FALSE
+  ) |> head(n = 5)

[1] 0.8425117 1.3281115 2.3309443 2.6794560 2.7939130

R> draw_sc_step_regular(
+    lambda_vector = 1:5, range_t = c(0.5, 5.9), atmost1 = FALSE,
+    atleast1 = FALSE
+  ) |> head(n = 5)

[1] 2.058468 2.100620 2.508954 3.125179 3.604882
```

Function `vdraw_sc_step_regular()` is a vectorized version of `draw_sc_step_regular()`. It returns a matrix with one event series per row, and as many columns as the maximum number of events across all draws.

```
R> vdraw_sc_step_regular(
+    lambda_matrix = matrix(runif(20), ncol = 5), range_t = c(1, 4),
+    atmost1 = FALSE
+  )

         [,1]     [,2]     [,3]     [,4]
[1,] 2.304123 2.802767       NA       NA
```

```
[2,] 2.990953       NA       NA       NA
[3,] 1.840374 2.134357 3.784424 3.816034
[4,] 2.136138 2.703826 3.269631       NA
```

The corresponding functions that return at least one event in the interval are `ztdraw_sc_step()`, `ztdraw_sc_step_regular()`, and `vztdraw_sc_step_regular()`.

5.2 Sampling NHPPPs with linear and log-linear intensities

Functions `draw_sc_linear()` and `ztdraw_sc_linear()` sample zero or more and at least one event, respectively, from NHPPPs with linear intensity functions. An optional argument (`atmost1`) returns the first event only.

$$\lambda(t) = \begin{cases} \alpha + \beta t & \text{for } t \in [a, b), t > -\frac{\alpha}{\beta} \\ 0 & \text{otherwise} \end{cases}.$$

```
R> draw_sc_linear(alpha = 3, beta = -0.5, range_t = c(0, 10)) |> head(n = 5)
```

```
[1] 0.3327657 0.4270154 0.5804320 0.6935027 0.9832093
```

```
R> ztdraw_sc_linear(alpha = 0.5, beta = 0.2, range_t = c(9.999, 10))
```

```
[1] 9.999757
```

An analogous set of functions (`[nhppp|ztnhppp]_sc_loglinear()`) samples from log-linear intensity functions

$$\lambda(t) = \begin{cases} e^{\alpha+\beta t} & \text{for } t \in [a, b) \\ 0 & \text{otherwise} \end{cases}.$$

The sampling algorithm is a variation of Algorithm 5, as described in [22]. Example usage follows.

```
R> draw_sc_loglinear(alpha = 1, beta = -0.02, range_t = c(8, 10))
```

```
 [1] 8.028806 8.128887 8.457669 8.483558 8.498647 8.503109 8.522725
 [8] 8.665979 8.671737 8.978065 8.981105 9.493691 9.815000 9.909167
```

```
R> ztdraw_sc_loglinear(alpha = 1, beta = -0.02, range_t = c(9, 10))

[1] 9.038160 9.075722 9.238302
```

6 Comparisons with other R packages

Table 3 lists five R packages that simulate from NHPPPs, including **nhppp**. We did not consider research code that is not an R package in the Comprehensive R Archive Network or is developed in other languages. For example, we do not run comparisons with the R and Python code for sampling from piecewise constant NHPPPs with regular time intervals in Garibay *et al* [23]. (Their code corresponds to the `vdraw_sc_step_regular()` function in **nhppp**.)

Package **reda** [24] focuses on recurrent event data analysis and can simulate NHPPPs with the inversion and thinning algorithms using the `simEvent()` function. It can take function object arguments for $\lambda(t)$. When using the thinning algorithm, it takes a constant majorizer. For the inversion algorithm, it approximates $\Lambda(t)$ and its inverse numerically, at a computational cost.

Package **simEd** [25] includes various functions for simulation education. Function `thinning()` implements the homonymous algorithm for drawing points from an NHPPP. Users can specify the intensity function and a piecewise constant or linear majorizer function.

Package **IndTestPP** [26] provides a framework for exploring the dependence between two or more realizations of point processes. It includes the ancillary function `simNHPc()` for simulating NHPPPs with the inversion or thinning algorithms. The function's argument is a piecewise constant approximation of the intensity function via a vector of evaluations, each corresponding to unit length subintervals. This resolution may not be adequate to simulate processes that change fast over a unit time interval.

Package **NHPoisson** [27, 28] fits NHPPP models to data and is not really geared towards mathematical simulation. Its `simNHP.fun()` function provides the ability for simulation-based inference via an implementation of the inversion algorithm. This function is designed to work with the package's inference machinery and is not practical to use for simulation, because the user has no direct control over the function's rescaling

of the time axis.

The claimed advantage of **nhppp** over the existing packages is that

- it samples from the target NHPPP and not from a numerical approximation thereof, e.g., as **IndTestPP** does.
- It can sample conditional on observing at least one event in the interval, which no other package implement.
- It accepts user-provided random number stream objects, which is useful for implementing simulation variance reduction techniques such as common random numbers [29] and antithetic variates [30].
- It is fast and memory efficient, both for the non-vectorized functions that are implemented in native `R` and for the vectorized functions that use `C++` plugins via the **Rcpp** package [31]. **nhppp** has specialized functions to leverage additional information about the point process, such as $\Lambda(t), \Lambda^{-1}(z)$, when available, which can result in faster simulation use the cumulative intensity function and its inverse, often at a computational speed advantage.

7 Illustrations

Depending on the application, we may have access to the intensity function or the integrated intensity function. We compared the `R` packages in Table 3 for sampling from a non-monotonic and highly non-linear intensity function for which the integrated intensity function can be derived analytically.

7.1 The target NHPPP to be simulated

Consider the example

$$\begin{aligned} \lambda(t) &= e^{rt}(1 + \sin wt), \\ \Lambda(t) &= \frac{e^{rt}(r \sin wt - w \cos wt) + w}{r^2 + w^2} + \frac{e^{rt} - 1}{r} \end{aligned} \tag{8}$$

of a sinusoidal intensity function $\lambda(t)$ scaled to have an exponential amplitude and one of its antiderivatives $\Lambda(t)$, with such a constant term that $\Lambda(0) = 0$. For the numerical

Table 3. NHPPP generation in `R` packages.

`R` package	Function	Algorithms (inputs)			Sample only earliest event	Custom RNG	Simulate given $N > 0$	Vectorized functions
		Thinning	Inversion	Order statistics				
nhppp	[see text]	$\lambda(t)$, $\lambda_*(t)$	$\Lambda(t), \Lambda^{-1}(z)$	$\Lambda(t), \Lambda^{-1}(z)$	Yes	**rstream** objects	Yes	For piecewise constant intensity
reda	`simEvent()`	$\lambda(t)$, λ_* constant	$\lambda(t)$ (no $\Lambda(t), \Lambda^{-1}(z)$)	No	Yes	No	No	No
simEd	`thinning()`	$\lambda(t)$, $[\lambda_{*m}]_{m=1}^{M}$	No	No	No	No	No	No
IndTestPP	`simNHPc()`	$[\lambda_m]_{m=1}^{M}$, λ_* constant	$[\lambda_m]_{m=1}^{M}$ (no $\Lambda(t), \Lambda^{-1}(z)$)	No	No	No	No	No
NHPoisson	`simNHP.fun()`	No	$\lambda(t)$, (no $\Lambda(t), \Lambda^{-1}(z)$)	No	No	No	No	No

RNG: random number generator object.

Fig 1. The $\lambda(t)$ (left) and $\Lambda(t)$ used in the illustration.

Also shown three majorizing functions (left panel, marked a, b, c) that are used with the thinning algorithm in the analyses.

study we set $r = 0.2$, $w = 1$, and $t \in (0, 6\pi]$. There is no analytic inverse function for this example. However, we can precompute `Li()`, a good numerical approximation to $\Lambda^{-1}(z)$. We will use it in Section 7.5 to compare the time performance of functions that use the inversion and order statistics algorithms when Λ^{-1} is available versus not.

```
R> l <- function(t) (1 + sin(t)) * exp(0.2 * t)
R> L <- function(t) {
+    exp(0.2 * t) * (0.2 * sin(t) - cos(t)) / 1.04 +
+      exp(0.2 * t) / 0.2 - 4.038462
+  }
R> Li <- approxfun(
+    x = L(seq(0, 6 * pi, 10^-3)),
+    y = seq(0, 6 * pi, 10^-3), rule = 2
+  )
```

Fig 1 graphs the intensity function and three majorizing functions over the interval of interest, which will be needed for the thinning algorithm.

The first, $\lambda_{*a}(t) = 43.38$, shown as a dashed blue line, is is a constant majorizer equal to the maximum of the intensity function. A constant majorizer may be a practical choice when only an upper bound is known for $\lambda(t)$. From (6), the analytic efficiency of the thinning algorithm using this majorizer is 0.209.

The second, $\lambda_{*b}(t)$, shown as a thin black line, is a piecewise constant envelope generated automatically from Algorithm A (in S1 Appendix) with 20 equal-length subintervals and Lipschitz cone coefficient $K = 52.05$. We set K equal to the maximum value of $|\frac{d\lambda(t)}{dt}|$ in the interval, attained at 6π. The analytic efficiency of the thinning algorithm using this majorizer is 0.245.

The third, $\lambda_{*c}(t)$, shown as a thicker black line, is a tighter piecewise constant majorizer with the same 20 equal-length subintervals that is constructed by finding a least upper bound in each subinterval. The analytic efficiency of the thinning algorithm

with the third majorizer is 0.718.

7.2 Simulation functions and algorithms

We sampled series of events from the target NHPPP using the packages and functions listed in Table 3. We repeated the sampling 10^4 times, recording all simulated points (event times). We also recorded the median computation time for drawing one series of events with single-threaded computation on modern hardware.

From the **nhppp** package we use

1. two functions that take as argument the intensity function and are based on Algorithm 4 (thinning): `draw_intensity()`, which uses linear majorizers such as λ_{*a}, and `draw_intensity_step()`, which uses piecewise constant majorizers such as λ_{*b} and λ_{*c} in the example.

2. Function `draw_cumulative_intensity_inversion()`, which takes as argument the cumulative intensity function $\Lambda(t)$ and is based on Algorithm 5 (time transformation/inversion), and

3. function `draw_cumulative_intensity_orderstats()`, which also uses $\Lambda(t)$ and is based on Algorithm 6 (order statistics).

Regarding the other `R` packages in Table 3, we used all except for **NHPoisson**, whose simulation function is tailored to supporting simulation based inference for data analysis and is not practical to use as a standalone function. (Its implementation does not allow the user to control the scaling of the time axis in a practical way.) However, its source code/algorithm is very similar to that of the **IndTestPP** simulation function, which is developed by the same authors.

We used the metrics in Table 4 to assess simulation performance with each function. We compared the empirical versus the simulated distributions of number of events and event times over $J = 100$ simulation runs.

7.3 Simulation performance with respect to number of events

We calculated the absolute and relative bias in the first two moments of the empirical distribution in the counts of events, the bounds of equal-tailed confidence intervals at

Table 4. Simulation metrics for the number of counts.

Metric	Definition	Description
Bias in mean	$B_\mu = \frac{1}{J}\sum_j n_j - N$	Mean difference from target in the number of counts.
Relative bias in mean	$B_{\mu,rel} = \frac{B_\mu}{N}$	Mean proportional difference from target in the number of counts.
Bias in variance	$B_V = \frac{1}{J}\sum_j \left(n_j - \frac{1}{J}\sum_j n_j\right)^2 - V$	Mean difference from target in variance of counts.
Relative bias in variance	$B_{V,rel} = \frac{B_V}{V}$	Mean proportional difference from target in variance of counts.
Equal-tailed p% confidence interval bounds	$n_{[p/2]}, n_{[1-p/2]}$	Quantiles of the empirical distribution of counts.
Goodness of fit p value	Statistic $\sum_x \frac{(O_x - E_x)^2}{E_x} \sim \chi^2_{U-L+1}$	Left-tail p value. p values near 1 imply good fit.
Wasserstein-1 distance	W_1, the smallest rearrangement of probability mass so that one distribution matches the other.	$W_1 = 0$ implies good fit
p value for $W_1 \neq 0$	Asymptotic theory p value	Two-sided p value. p values near 1 imply good fit.

In the Table, $j \in [J]$ indexes simulations, n_j is the number of counts in simulation j, $N = \Lambda(6\pi) - \Lambda(0)$ is the theoretical mean number of counts, and $V = \Lambda(6\pi) - \Lambda(0) = N$ the theoretical variance. The lower and upper bounds of an equal-tailed p% confidence interval, $p \in \{95, 90, 75, 50\}$, are denoted with $n_{[p/2]}, n_{[1-p/2]}$, respectively. For the goodness of fit, we created bins $[0, L), [L, L+1), \ldots, [U, \infty)$, where L, U are the 0.001 and 0.999 percentiles of the Poisson distribution with parameter $\Lambda(6\pi) - \Lambda(0)$. We indexed bins with $x \in \{1, \ldots, U - L + 2\}$. The goodness of fit statistic contrasts the observed (O_x) versus expected (E_x) numbers of events over the bins and it is compared with a χ^2_{U-L+1} distribution to obtain a p value.

the 95, 90, 75, and 50 percent levels, a χ^2-distributed goodness of fit statistic and its p-value, and the Wasserstein-1 distance W_1 between the empirical and the theoretical count distributions and the asymptotic one sided p value to reject whether $W_1 = 0$ according to [32]. W_1 is the smallest mass that has to be redistributed so that one distribution matches the other. W_1 is equal to the unsigned area between the cumulative distribution functions of the compared distributions. For example, $W_1 = 5.25$ means that the mass that must be moved to transform one density to the other is no less than 5.25 counts and a $W_1 = 0$ implies perfect fit.

The results for the **nhppp** functions in Fig 2 and Table 5 suggest excellent simulation performance.

The respective results for the `R` packages are in Fig 3 and Table 6. The simulation performance with the **reda** functions is excellent. Performance with **simEd** and

Fig 2. Theoretical (red) and empirical (black) cumulative distribution functions for event counts in the illustration example with nhppp functions.

The unsigned area between the theoretical and empirical curves equals the Wasserstein-1 distance in Table 5.

Table 5. Simulated total number of events with nhppp functions for the illustration example.

	Thinning $\lambda_*=\lambda_{*a}$	Thinning $\lambda_*=\lambda_{*b}$	Thinning $\lambda_*=\lambda_{*c}$	Inversion	Order statistics
Sample mean	171.057	171.257	171.322	171.193	171.131
B_μ	-0.078	0.122	0.187	0.058	-0.004
$B_{\mu,rel}$	-0.045	0.071	0.109	0.034	-0.002
Sample variance	175.015	168.218	173.918	166.950	166.933
B_V	3.880	-2.917	2.783	-4.185	-4.201
$B_{V,rel}$	2.267	-1.704	1.626	-2.445	-2.455
Goodness of fit, χ^2 [p value]	0.145 [1.000]	0.160 [1.000]	0.117 [1.000]	0.384 [1.000]	0.229 [1.000]
W_1 [p value]	0.194 [1.000]	0.189 [1.000]	0.231 [0.997]	0.195 [1.000]	0.187 [1.000]
Equal tail 95% CI = [146, 197]	[146, 197]	[146, 197]	[146, 197]	[146, 197]	[146, 197]
Equal tail 90% CI = [150, 193]	[150, 193]	[150, 193]	[150, 193]	[150, 193]	[150, 193]
Equal tail 75% CI = [156, 186]	[156, 186]	[156, 186]	[156, 187]	[156, 186]	[156, 186]
Equal tail 50% CI = [162, 180]	[162, 180]	[162, 180]	[162, 180]	[162, 180]	[162, 180]

Equal tail p% CI: a confidence interval whose bounds are the $p/2$ and $(1-p/2)$ count percentiles of the respective cumulative distribution function.

IndTestPP functions depends on the adequacy with which they approximate the target density. In this example, the approximation accuracy is not ideal for either package, but is somewhat worse for **IndTestPP**.

Fig 3. Theoretical (red) and empirical (black) cumulative distribution functions for event counts in the illustration example with the `R` packages in Table 3.

The unsigned area between the theoretical and empirical curves equals the Wasserstein-1 distance in Table 5.

7.4 Event times

We compared the theoretical and empirical distribution of event times for all $J = 10^4$ event time draws. We calculated a goodness of fit statistic by binning realized times in 70 bins and its p value, by comparing the statistic against the χ^2_{69} distribution. We also calculated the W_1 distance between these distributions and its associated p value.

Fig 4 and Table 7 indicate excellent simulation performance with the **nhppp** functions.

Fig 5 and Table 8 indicate excellent simulation performance with the **reda** functions.

Table 6. Simulated total number of events with the R packages of Table 3 for the illustration example.

	reda thinning, $\lambda_*=\lambda_{*a}$	**reda** inversion	**simEd** thinning, $\lambda_*=\lambda_{*a}$	**IndTestPP** thinning, no λ_*	**IndTestPP** inversion
Sample mean	172.430	174.170	179.910	190.490	191.030
B_μ	1.295	3.035	8.775	19.355	19.895
$B_{\mu,rel}$	0.757	1.774	5.128	11.310	11.626
Sample variance	168.429	145.193	155.355	194.838	191.484
B_V	-2.705	-25.942	-15.779	23.704	20.349
$B_{V,rel}$	-1.581	-15.159	-9.220	13.851	11.891
Goodness of fit, χ^2 [p value]	6.830 [1.000]	10.720 [1.000]	67.482 [0.994]	226.107 [<0.001]	237.199 [<0.001]
W_1 [p value]	1.453 [0.256]	3.083 [0.112]	8.856 [<0.001]	19.356 [0.086]	19.896 [0.170]
Equal tail 95% CI = [146, 197]	[152, 199]	[152, 196]	[161, 203]	[163, 214]	[168, 217]
Equal tail 90% CI = [150, 193]	[154, 195]	[154, 192]	[161, 203]	[167, 214]	[170, 215]
Equal tail 75% CI = [156, 186]	[158, 189]	[161, 187]	[169, 202]	[174, 205]	[176, 207]
Equal tail 50% CI = [162, 180]	[162, 181]	[165, 180]	[170, 183]	[178, 201]	[181, 200]

Equal tail p% CI: a confidence interval whose bounds are the $p/2$ and $(1-p/2)$ count percentiles of the respective cumulative distribution function.

Fig 4. Simulated event times with nhppp.

Left column: histogram (gray) and theoretical distribution (red) of event times; right column: empirical (black) and theoretical (red) cumulative distribution function. The unsigned area between the empirical and cumulative distribution functions is the W_1 distance in Table 7.

Table 7. Goodness of fit of simulated event times with nhppp functions for the example.

	Goodness of fit, χ^2 [p value]	W_1 [p value]
Thinning $\lambda_*=\lambda_{*a}$	0.004 [1.000]	0.396 [1.000]
Thinning $\lambda_*=\lambda_{*b}$	0.004 [1.000]	0.361 [1.000]
Thinning $\lambda_*=\lambda_{*c}$	0.004 [1.000]	0.338 [1.000]
Inversion	0.004 [1.000]	0.347 [1.000]
Order statistics	0.004 [1.000]	0.350 [1.000]

The simulation performance with the **simEd** and **IndTestPP** functions, which rely on approximations, is not as good.

Table 8. Goodness of fit of simulated event times with R functions in Table 3.

	Goodness of fit, χ^2 [p value]	W_1 [p value]
reda thinning ($\lambda_*=\lambda_{*a}$)	0.012 [1.000]	0.356 [1.000]
reda inversion	0.010 [1.000]	0.354 [1.000]
simEd thinning ($\lambda_*=\lambda_{*a}$)	0.028 [1.000]	0.338 [0.990]
IndTestPP thinning (no λ_*)	0.460 [1.000]	2.152 [0.930]
IndTestPP inversion	0.490 [1.000]	2.372 [0.927]

Fig 5. Simulated event times with the `R` packages in Table 3.

Left column: histogram (gray) and theoretical distribution (red) of event times; right column: empirical (black) and theoretical (red) cumulative distribution function. The unsigned area between the empirical and cumulative distribution functions is the W_1 distance in Table 8.

7.5 Time performance

7.5.1 Time performance of non-vectorized functions

To indicate time performance, we benchmarked functions by recording execution times when drawing a series of points (Fig 6). We also benchmarked functions for drawing the first-occurring event, because **nhppp** functions can sample the first time more efficiently when the inversion algorithm is used (Fig 7).

Fig 6. Computation times when drawing all events in interval.

Fig 7. Computation times when drawing the first event in interval.

We provided functions with the arguments they need to run fastest. For example, functions that use the inversion or order statistics algorithm execute faster when the inverse function $\Lambda^{-1}(z)$ is provided, rather than numerically calculated, as shown in both Figures for the **nhppp** package. (Functions in other packages do not take $\Lambda(t)$ and $\Lambda^{-1}(z)$ arguments.) The fastest functions are **nhppp** functions that rely on the inversion or order statistics algorithms given $\Lambda^{-1}(z)$.

According to (6), the thinning algorithm has higher efficiency, and is expected to execute faster, for majorizer functions that envelop the intensity function more closely. Observe that $\lambda_{*a} \succ \lambda_{*c}$ and $\lambda_{*b} \succ \lambda_{*c}$ in Fig 1. As expected, the execution times are indeed shorter for majorizer 'c' compared to 'b' in Figures 6 and 7. However, the execution times are longer with majorizer 'c' compared to 'a' because `draw_intensity()`, the function that uses constant majorizers, and `draw_intensity_step()`, the function that use piecewise constant majorizers, are implemented differently. `draw_intensity()` happens to be faster in this example, but this is not always true.

In **nhppp**, functions that use the inversion or order statistics algorithms can exit earlier when only the first event is requested. This is not possible, however, for the

thinning algorithm. This efficiency does not appear to be implemented in the other packages.

7.5.2 Time performance of vectorized functions

In `R`, 'vectorized' computation, where operations are done in columns, is faster than using `for` loops or `apply()` functions. As shown in Table 1, **nhppp** includes vectorized functions for sampling from (i) piecewise constant intensity functions, using `[vdraw|vztdraw]_sc_step_regular()`; and (ii) general intensity functions, using `[vdraw|vztdraw]_intensity_step_regular()`.

We compared the execution speed of non-vectorized and vectorized functions for sampling 10^5 times from the piecewise constant 'b' majorizer (λ_{*b}) in Fig 1. The expected number of events with λ_{*b} in $(0, 6\pi]$ is 741.97. When drawing only the earliest event, the vectorized function is approximately 113 times faster than the non-vectorized function (median $59ms$ versus $6717ms$ over 10^5 simulations). When drawing all events , the vectorized function is approximately 1.4 times faster than the non-vectorized function (median $36.55s$ versus $50.97s$ over 10^5 simulations). The reason that the difference in speed attenuates is that the current implementation of the vectorized functions does not use sparse matrices to store samples, which introduces inefficiencies the expected number of samples becomes larger.

8 Summary and next developments

The **nhppp** facilitates the simulation of NHPPPs from time-varying intensity or cumulative intensity functions. Its claim is that it (i) simulates correctly from a target density, not just from an approximation; (ii) samples conditional on observing at least one event in an interval; (iii) accomodates user provided random number stream objects; and (iv) is fast. The current version includes one vectorized function for sampling from regular-spaced piecewise constant intensity functions. In future releases we will further optimize execution speed and memory usage.

Computational details and credits

R 4.3.1 [33] was used for all analyses. Packages **xtable** 1.8.4 [34] and **knitr** 1.45 [35] were used for automatic report generation. Packages **ggplot2** 3.4.4 [36], **ggridges** 0.5.5 [37], and **latex2exp** 0.9.6 [38] were used for plot generation and LaTeXformatting. Packages **nhppp** 0.1.4 [16], **bench** 1.1.3 [39], **rstream** 1.3.7 [40], **otinference** 0.1.0 [41], and **parallel** 4.3.1 were used in the examples and the analyses.

All computations were done on an Apple M1 Max machine with 64 megabytes of random access memory. A preprint of the current paper is in [17]. R itself and all aforementioned packages are available from the Comprehensive R Archive Network (CRAN) at `https://CRAN.R-project.org/`.

Supporting information

S1 Appendix. Piecewise constant majorizer functions. Algorithm for the automatic generation of piecewise constant majorizer functions.

S2 Appendix. Conditional sampling from NHPPPs. Algorithm to sample conditionally on observing at least m events in $(a, b]$.

S3 R code. Code to reproduce the exhibits. R code to reproduce the exhibits. Timing results are machine and platform specific.

Acknowledgments

This work was funded from grant U01CA265750 from the National Cancer Institute. We thank the investigators of the Cancer Incidence and Surveillance Modeling Network (CISNET) Bladder Cancer Site Stavroula Chrysanthopoulou, Jonah Popp, Fernando Alarid-Escudero, Hawre Jalal, and David Garibay for useful discussions.

References

1. Law AM, Kelton WD, Kelton WD. Simulation modeling and analysis. vol. 3. Mcgraw-hill New York; 2007.

2. Luchak G. The solution of the single-channel queuing equations characterized by a time-dependent Poisson-distributed arrival rate and a general class of holding times. Operations Research. 1956;4(6):711–732.

3. Kim SH, Whitt W. Choosing arrival process models for service systems: Tests of a nonhomogeneous Poisson process. Naval Research Logistics (NRL). 2014;61(1):66–90.

4. Yang W, Su Q, Huang SH, Wang Q, Zhu Y, Zhou M. Simulation modeling and optimization for ambulance allocation considering spatiotemporal stochastic demand. Journal of Management Science and Engineering. 2019;4(4):252–265.

5. Zhou Z, Matteson DS, Woodard DB, Henderson SG, Micheas AC. A spatio-temporal point process model for ambulance demand. Journal of the American Statistical Association. 2015;110(509):6–15.

6. Abdel-Aty MA, Radwan AE. Modeling traffic accident occurrence and involvement. Accident Analysis & Prevention. 2000;32(5):633–642.

7. Thompson W. On the foundations of reliability. Technometrics. 1981;23(1):1–13.

8. England T, Harper P, Crosby T, Gartner D, Arruda EF, Foley K, et al. Modelling lung cancer diagnostic pathways using discrete event simulation. Journal of Simulation. 2023;17(1):94–104.

9. Rutter CM, Savarino JE. An evidence-based microsimulation model for colorectal cancer: validation and application. Cancer Epidemiol Biomarkers Prev. 2010;19(8):1992–2002. doi:10.1158/1055-9965.Epi-09-0954.

10. Jeon J, Meza R, Moolgavkar SH, Luebeck EG. Evaluation of screening strategies for pre-malignant lesions using a biomathematical approach. Math Biosci. 2008;213(1):56–70. doi:10.1016/j.mbs.2008.02.006.

11. Tsokos CP, Xu Y. Non-homogenous Poisson Process for Evaluating Stage I & II Ductal Breast Cancer Treatment. Journal of Modern Applied Statistical Methods. 2011;10(2):646–655. doi:10.22237/jmasm/1320121320.

12. Andreev VP, Head T, Johnson N, Deo SK, Daunert S, Goldschmidt-Clermont PJ. Discrete event simulation model of sudden cardiac death predicts high impact of preventive interventions. Scientific reports. 2013;3(1):1771.

13. Getsios D, Blume S, Ishak KJ, Maclaine GD. Cost effectiveness of donepezil in the treatment of mild to moderate Alzheimer's disease: a UK evaluation using discrete-event simulation. Pharmacoeconomics. 2010;28:411–427.

14. Mar J, Soto-Gordoa M, Arrospide A, Moreno-Izco F, Martínez-Lage P. Fitting the epidemiology and neuropathology of the early stages of Alzheimer's disease to prevent dementia. Alzheimer's research & therapy. 2015;7:1–8.

15. Zhang X. Application of discrete event simulation in health care: a systematic review. BMC health services research. 2018;18:1–11.

16. Trikalinos TA, Sereda Y. **nhppp**: Simulating Nonhomogeneous Poisson Point Processes in `R`; 2024. Available from: `https://CRAN.R-project.org/package=nhppp`.

17. Trikalinos TA, Sereda Y. **nhppp**: Simulating Nonhomogeneous Poisson Point Processes in `R`; 2024.

18. Cox D, Miller H. The Poisson Process. In: The Theory of Stochastic Processes. Chapman and Hall; 1965. p. 147.

19. Lewis PW, Shedler GS. Simulation of nonhomogeneous Poisson processes by thinning. Naval Research Logistics Quarterly. 1979;26(3):403–413.

20. Çinlar E. Introduction to stochastic processes Prentice-Hall. Englewood Cliffs, New Jersey (420p); 1975.

21. Press W, Teukolsky S, Vetterling W, Flannery B. Section 9.3. Van Wijngaarden-Dekker-Brent Method. Numerical Recipes: The Art of Scientific Computing. Cambridge University Press, New York; 2007.

22. Lewis P, Shedler G. Simulation of nonhomogeneous Poisson processes with log linear rate function. Biometrika. 1976;63(3):501–505.

23. Garibay D, Jalal H, Alarid-Escudero F. A computationally efficient nonparametric sampling (NPS) method of time to event for individual-level models. medRxiv. 2024;doi:10.1101/2024.04.05.24305356.

24. Wang W, Fu H, Yan J. **reda**: Recurrent Event Data Analysis; 2022. Available from: `https://github.com/wenjie2wang/reda`.

25. Lawson B, Leemis L, Kudlay V. **simEd**: Simulation Education; 2023. Available from: `https://CRAN.R-project.org/package=simEd`.

26. Cebrián AC. **IndTestPP**: Tests of Independence and Analysis of Dependence Between Point Processes in Time; 2020. Available from: `https://CRAN.R-project.org/package=IndTestPP`.

27. Cebrián AC, Abaurrea J, Asín J. **NHPoisson**: An `R` Package for Fitting and Validating Nonhomogeneous Poisson Processes. Journal of Statistical Software. 2015;64(6):1–25. doi:10.18637/jss.v064.i06.

28. Cebrián AC. **NHPoisson**: Modelling and Validation of Non-Homogeneous Poisson Processes; 2020. Available from: `https://CRAN.R-project.org/package=NHPoisson`.

29. Wright R, Ramsay Jr T. On the effectiveness of common random numbers. Management Science. 1979;25(7):649–656.

30. Hammersley JM, Mauldon JG. General principles of antithetic variates. In: Mathematical proceedings of the Cambridge philosophical society. vol. 52. Cambridge University Press; 1956. p. 476–481.

31. Eddelbuettel D, Francois R, Allaire J, Ushey K, Kou Q, Russell N, et al.. **Rcpp**: Seamless `R` and `C++` Integration; 2024. Available from: `https://CRAN.R-project.org/package=Rcpp`.

32. Sommerfeld M, Munk A. Inference for empirical Wasserstein distances on finite spaces. Journal of the Royal Statistical Society Series B: Statistical Methodology. 2018;80(1):219–238.

33. R Core Team. R: A Language and Environment for Statistical Computing; 2023. Available from: https://www.R-project.org/.

34. Dahl DB, Scott D, Roosen C, Magnusson A, Swinton J. **xtable**: Export Tables to LaTeXor HTML; 2019. Available from: https://CRAN.R-project.org/package=xtable.

35. Xie Y. **knitr**: A Comprehensive Tool for Reproducible Research in **R**. In: Stodden V, Leisch F, Peng RD, editors. Implementing Reproducible Computational Research. Chapman and Hall/CRC; 2014.

36. Wickham H. **ggplot2**: Elegant Graphics for Data Analysis. Springer-Verlag New York; 2016. Available from: https://ggplot2.tidyverse.org.

37. Wilke CO. **ggridges**: Ridgeline Plots in **ggplot2**; 2023. Available from: https://CRAN.R-project.org/package=ggridges.

38. Meschiari S. **latex2exp**: Use LaTeXExpressions in Plots; 2022. Available from: https://CRAN.R-project.org/package=latex2exp.

39. Hester J, Vaughan D. **bench**: High Precision Timing of R Expressions; 2023. Available from: https://CRAN.R-project.org/package=bench.

40. Leydold J. **rstream**: Streams of Random Numbers; 2022. Available from: https://CRAN.R-project.org/package=rstream.

41. Sommerfeld M. **otinference**: Inference for Optimal Transport; 2017. Available from: https://CRAN.R-project.org/package=otinference.

Fig 1

Click here to access/download;Figure;Fig1.tif

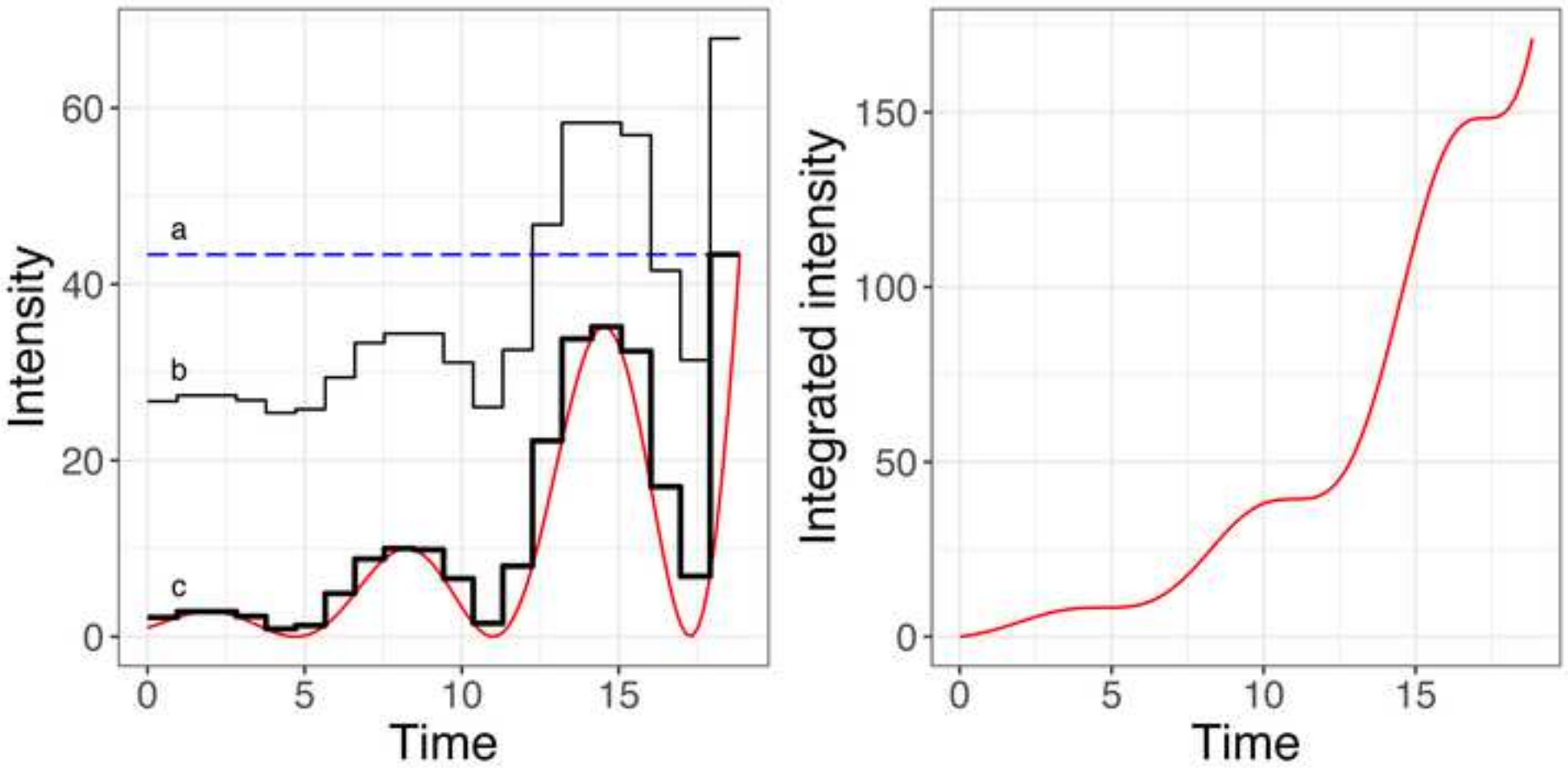

Fig 2

Click here to access/download;Figure;Fig2.tif

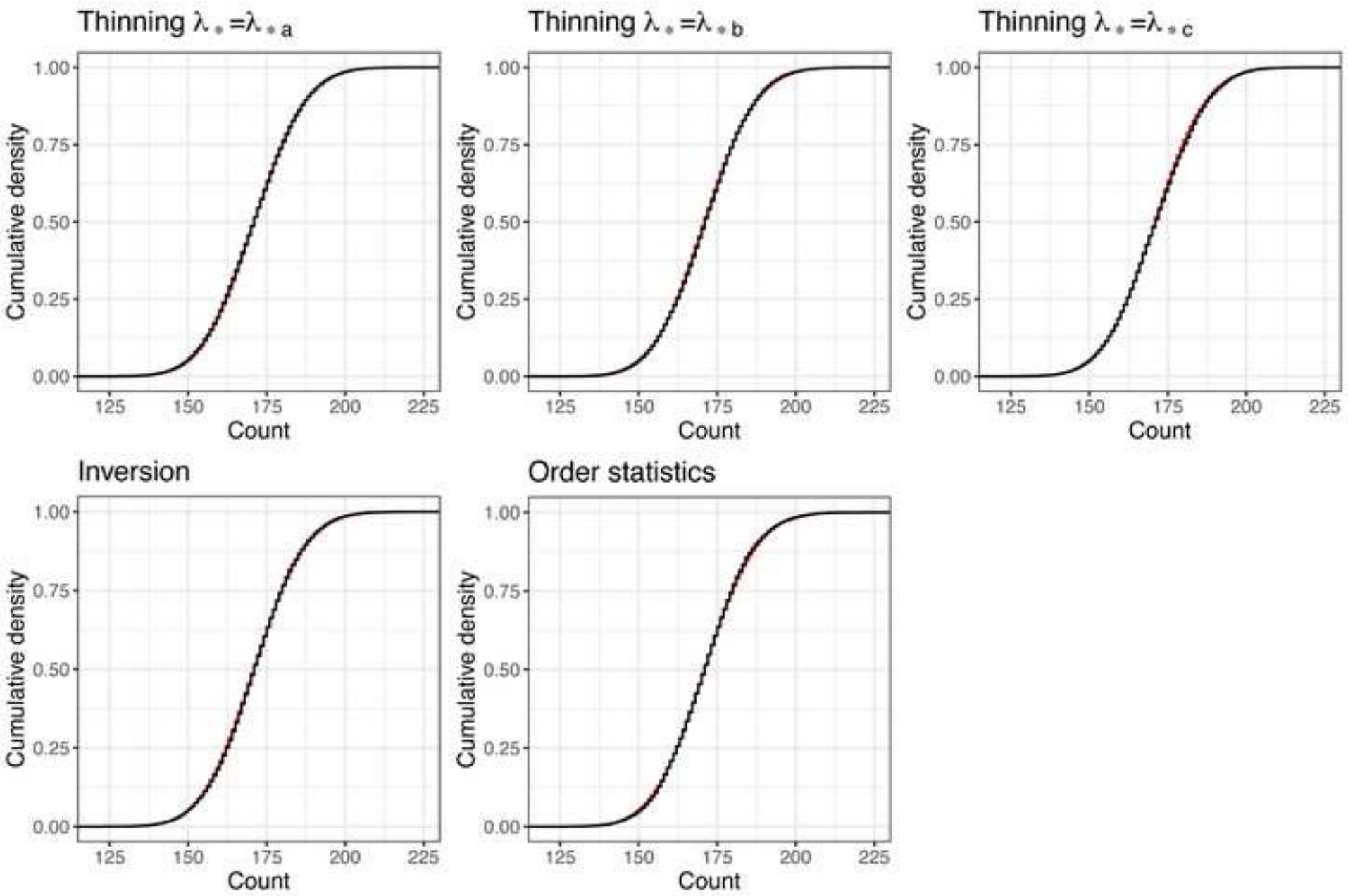

Fig 3

Click here to access/download;Figure;Fig3.tif

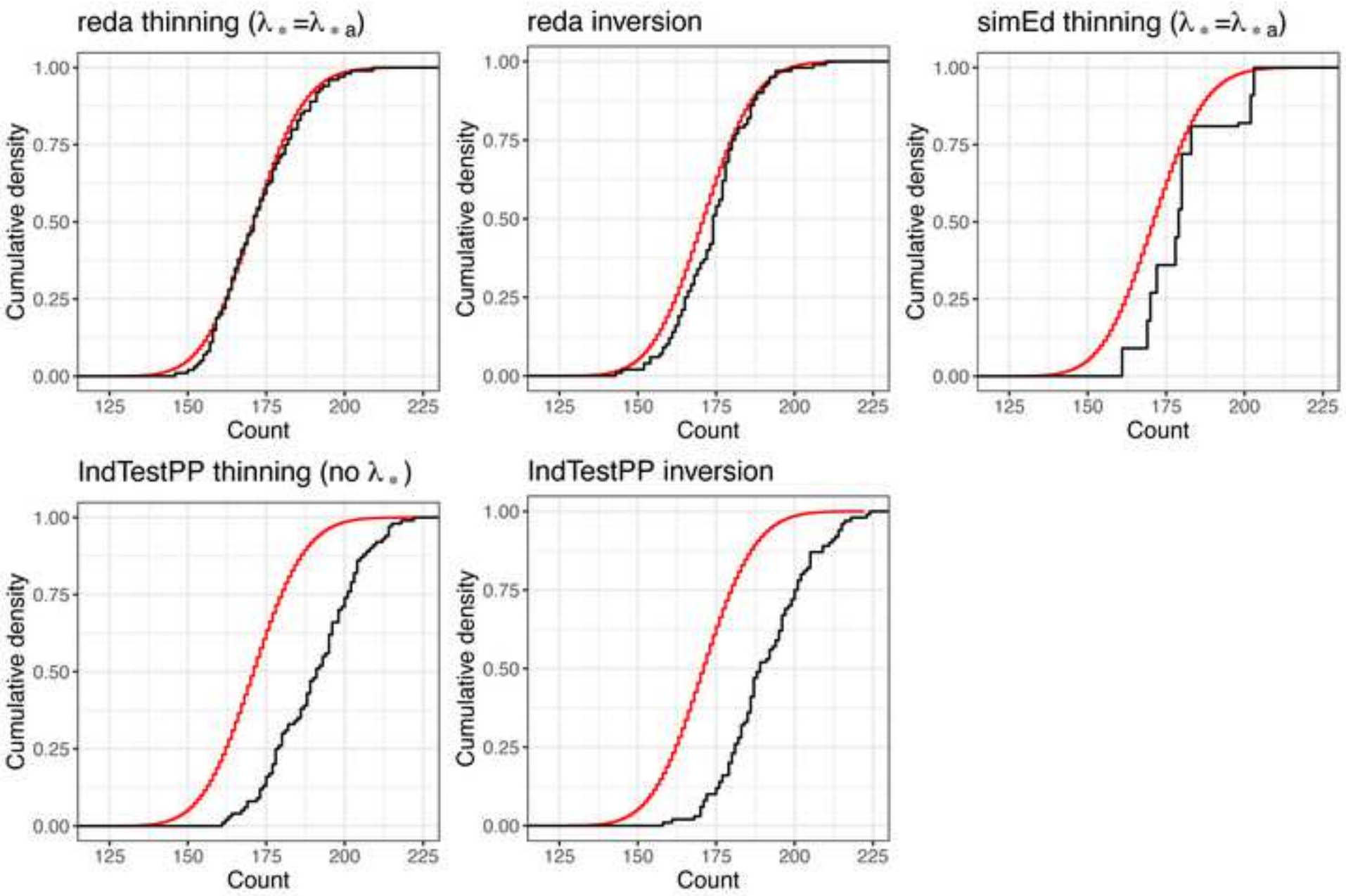

Fig 4

Click here to access/download;Figure;Fig4.tif

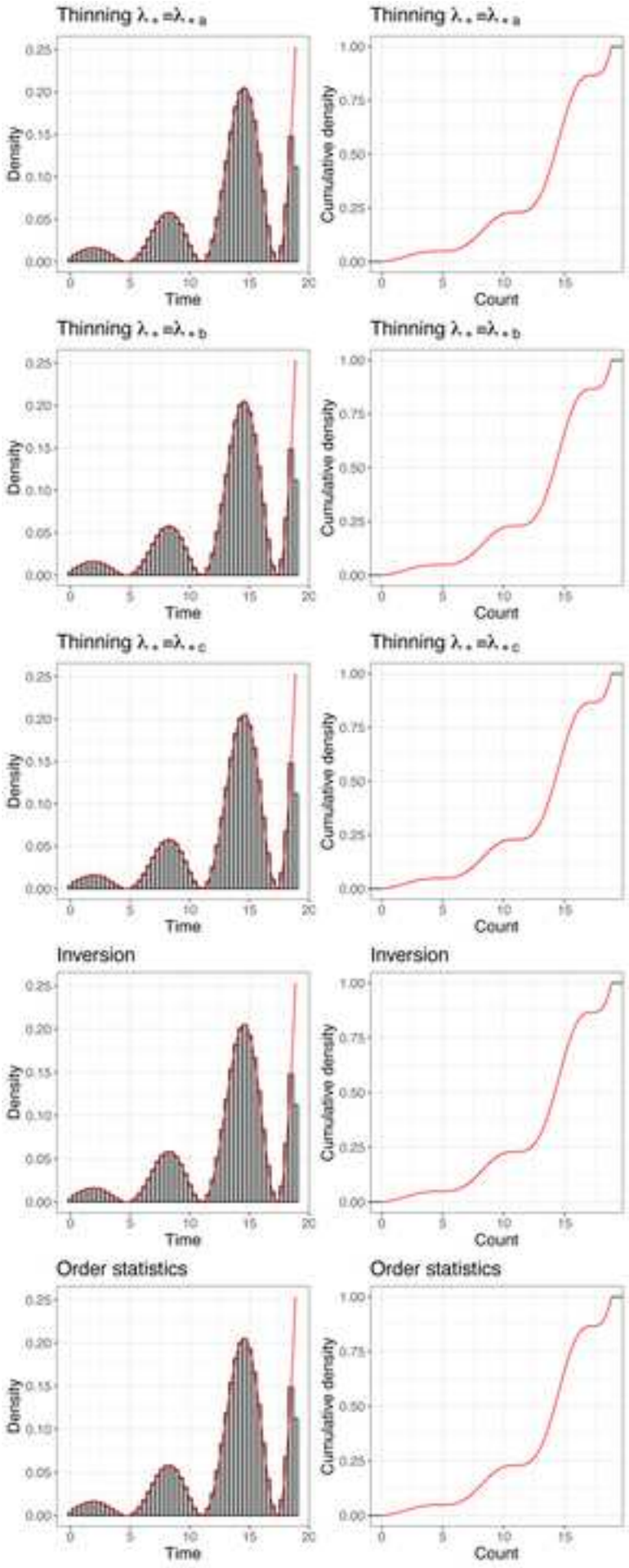

Fig 5

Click here to access/download;Figure;Fig5.tif

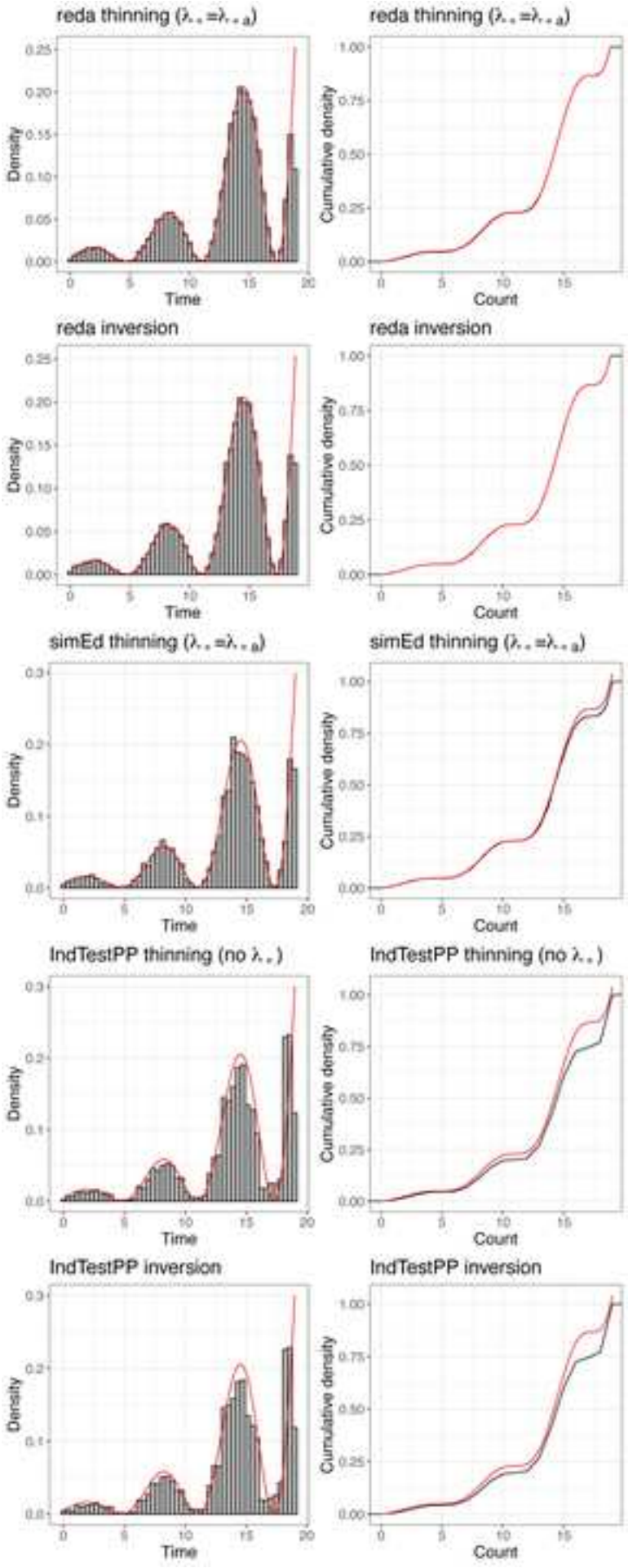

Fig 6

Click here to access/download;Figure;Fig6.tif

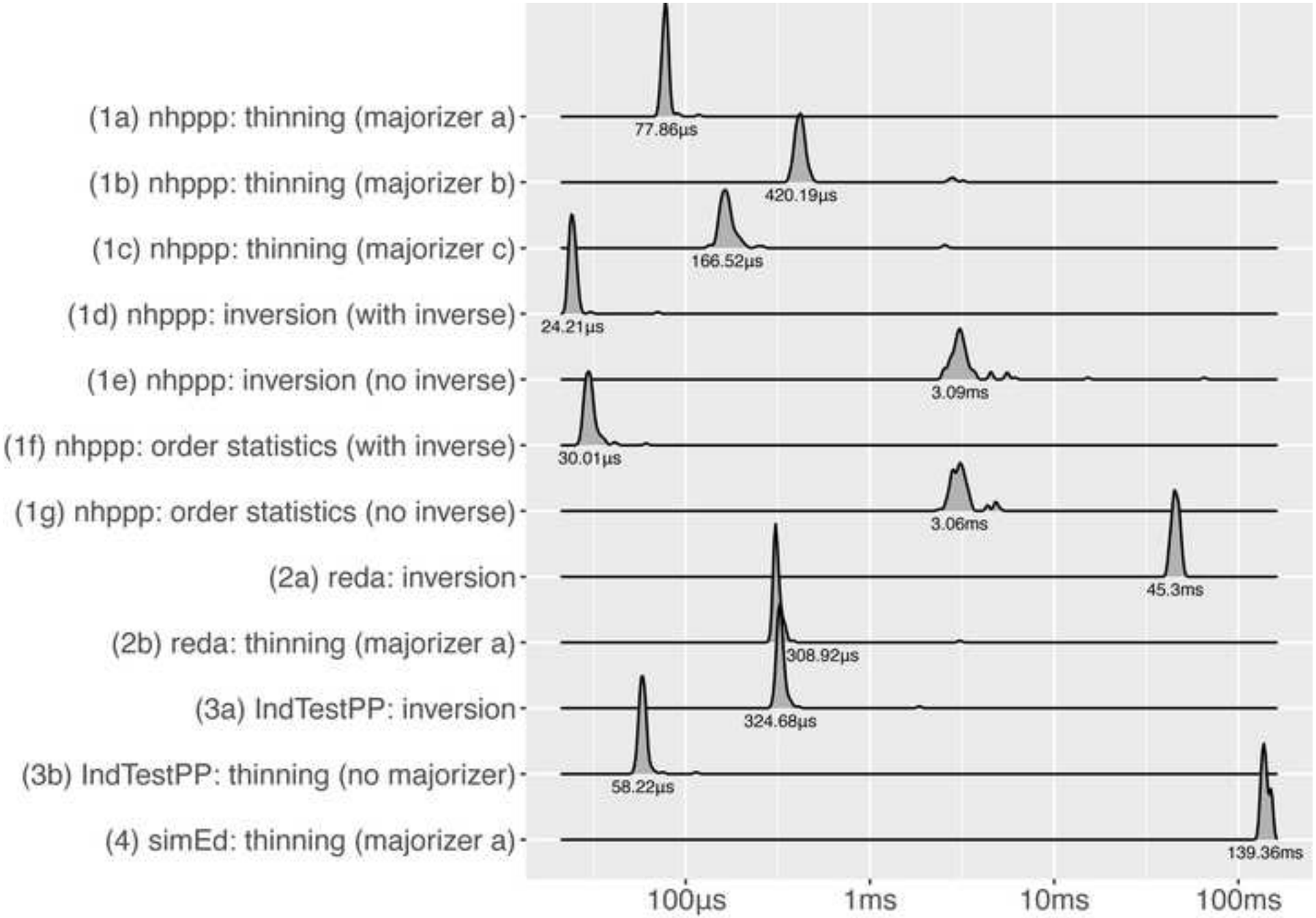

Fig 7

Click here to access/download;Figure;Fig7.tif

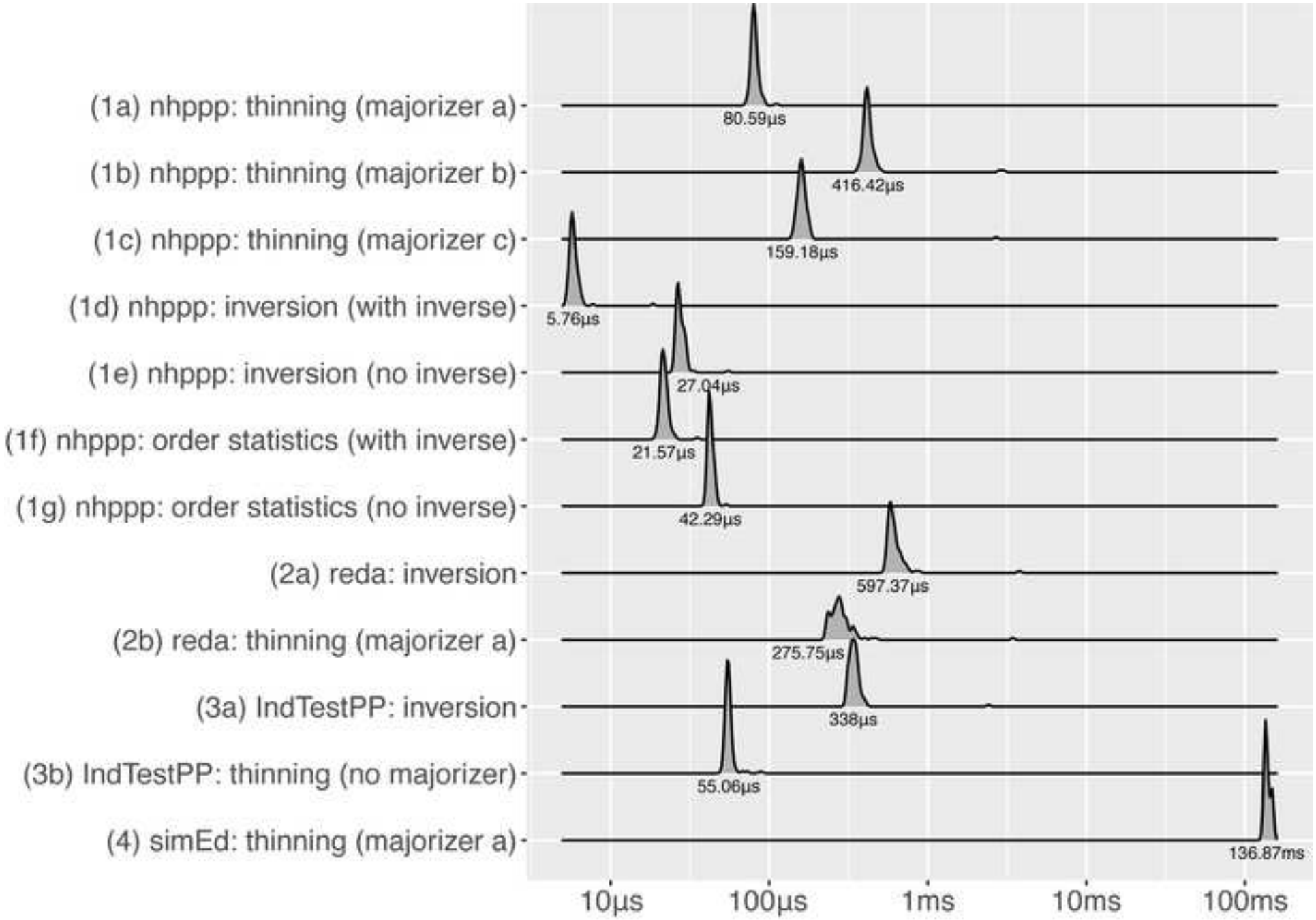

Click here to access/download
Supporting Information
S1Appendix.pdf

Click here to access/download
Supporting Information
S2Appendix.pdf

Supporting Information S3 Appendix R code

Click here to access/download
Supporting Information
S3Code.R.txt

Click here to access/download
Other
arXiv_preprint.pdf

Revised Manuscript with Track Changes

The **nhppp** package for simulating non-homogeneous Poisson point processes in R

Thomas A. Trikalinos[1,2,3,*], Yuliia Sereda[1]

1 Center for Evidence Synthesis in Health, Brown University, Providence, RI, USA

2 Department of Health Services, Policy & Practice, Brown University, Providence, RI, USA

3 Department of Biostatistics, Brown University, Providence, RI, USA

* thomas_trikalinos@brown.edu

Abstract

We introduce the **nhppp** package for simulating events from one dimensional non-homogeneous Poisson point processes (NHPPPs) in R fast and with a small memory footprint. We developed it to facilitate the sampling of event times in discrete event and statistical simulations. The package's functions are based on three algorithms that provably sample from a target NHPPP: the time-transformation of a homogeneous Poisson process (of intensity one) via the inverse of the integrated intensity function; the generation of a Poisson number of order statistics from a fixed density function; and the thinning of a majorizing NHPPP via an acceptance-rejection scheme. We present a study of numerical accuracy and time performance of the algorithms. We illustrate use with simple reproducible examples.

1 Introduction

It is often desirable to simulate series of events (stochastic point processes) so that the intensity of their occurrence varies over time. Examples include events such as the occurrence of death and occurrences of symptoms, infections, or tumors over a person's lifetime. The non-homogeneous Poisson point process (NHPPP), which generalizes the simpler homogeneous-Poisson, Weibull, and Gompertz point processes, is a widely used model for such series of events. NHPPPs can model complicated event patterns given a suitable intensity function. They are, therefore, useful in statistical and mathematical model simulation.

An NHPPP has the properties that the number of events in all non-overlapping time intervals are independent random variables and that, within each time interval, the number of events is Poisson distributed. Thus an NHPPP is a memoryless point process. A large number of phenomena may reasonably conform with these properties.

NHPPPs have been used in the simulation analysis of queues in queuing theory and operations research [1, 2]; hospital operations [3]; ambulance services [4, 5]; traffic accidents [6]; product and network reliability [7]; and the modeling of cancer [8–11], heart disease [12], and dementia [13, 14], among other applications [15]. NHPPPs are used so widely in part because their assumptions are often plausible. For example, when modeling traffic accidents along a road, it may be plausible to assume that individual accidents are independent of each other, but they happen in some locations more often because the probability of an accident depends on local aspects of the road, such as turns, slopes, and propensity for slippery conditions. Similarly, when modeling the impact of screening strategies on colorectal cancer outcomes at the population level, it is probably plausible to assume that, for each person, the emergence of precancerous lesions (adenomas) over a time interval is independent of whether such lesions emerged in other non-overlapping time intervals. In these examples, the intensity of event occurrence over the carrier space (the probability of a traffic accident along a road; and the probability that an adenoma will emerge in a person's colon at different ages) is captured by the NHPPP's intensity function. An NHPPP can model complicated event patterns using intensity functions that vary over the carrier space (e.g., length of road, time).

The **nhppp** package in `R` contains functions for the simulation of NHPPPs over a one-dimensional carrier space, which we will take to represent time [16, 17]. Table 1 summarizes the functions implemented in **nhppp** as of version 0.1.4. You can install the development version of **nhppp** with

```
R> # install.packages("devtools")
R> devtools::install_github("bladder-ca/nhppp")
```

or the release version with

```
R> install.packages("nhppp")
```

We review NHPPPs in Section 2 and algorithms for sampling from constant rate Poisson point processes in Section 3. We introduce the three sampling algorithms that are implemented in the package in Section 4. We discuss special functional forms for the intensity function (constant, piecewise constant, linear, and log-linear) in Section 5. We describe **nhppp** versus other `R` packages that can simulate from one dimensional NHPPPs in Section 6 and present a numerical study in Section 7. We summarize in Section 8.

2 The Poisson point process

2.1 Definition

The Poisson point process is a stochastic series of events on the real line. For some sequence of events, let $N(t, t+\Delta t)$ be the number of events in the interval $(t, t+\Delta t]$. If for some positive intensity λ and, as $\Delta t \to 0$,

$$\begin{aligned} \Pr[N(t,t+\Delta t)=0] &= 1-\lambda\Delta t + o(\Delta t), \\ \Pr[N(t,t+\Delta t)=1] &= \lambda\Delta t + o(\Delta t), \\ \Pr[N(t,t+\Delta t)>1] &= o(\Delta t), \text{ and} \\ N(t,t+\Delta t) &\perp\!\!\!\perp N(0,t), \end{aligned} \tag{1}$$

then that sequence of events is a Poisson point process. In Equation (1), the third statement demands that events occur one at a time. The fourth statement implies that

Table 1. Functions in nhppp.

Intensity function	Function name	Function simulates...
Constant	`ppp_n()`	exactly n events in $[a, b)$
	`ppp_next_n()`	the next n events in $[a, \infty)$
	`ppp_sequential()`, `ppp_orderstat()`	≥ 0 events in $[a, b)$
	`ztppp()`	≥ 1 events in $[a, b)$
Time-varying, special cases, non-vectorized	`draw_sc_linear()`	≥ 0 events in $[a, b)$ from $\lambda(t) = \alpha + \beta t$
	`draw_sc_loglinear()`	≥ 0 events in $[a, b)$ from $\lambda(t) = \exp(\alpha + \beta t)$
	`draw_sc_step()`	≥ 0 events in $[a, b)$ from piecewise constant $\lambda(t)$ with uneven intervals
	`draw_sc_step_regular()`	≥ 0 events in $[a, b)$ from piecewise constant $\lambda(t)$ with regular intervals
	`ztdraw_sc_linear()`	≥ 1 events in $[a, b)$ from $\lambda(t) = \alpha + \beta t$
	`ztdraw_sc_loglinear()`	≥ 1 events in $[a, b)$ from $\lambda(t) = \exp(\alpha + \beta t)$
Time varying, special cases, vectorized	`vdraw_sc_step_regular()`	≥ 0 events in $[a, b)$ from piecewise constant $\lambda(t)$ with regular intervals
	`vztdraw_sc_step_regular()`	≥ 1 events in $[a, b)$ from piecewise constant $\lambda(t)$ with regular intervals
Time-varying, general case, non-vectorized	`draw()`	(wrapper function)
	`draw_cumulative_intensity_inversion()`	≥ 0 events in $[a, b)$ from $\Lambda(t), \Lambda^{-1}(t)$
	`draw_cumulative_intensity_orderstats()`	≥ 0 events in $[a, b)$ from $\Lambda(t), \Lambda^{-1}(t)$
	`draw_intensity()`	≥ 0 events in $[a, b)$ from $\lambda(t), \lambda_*(t)$
	`draw_intensity_step()`	≥ 0 events in $[a, b)$ from $\lambda(t)$ and piecewise constant $\lambda_*(t)$
	`ztdraw_cumulative_intensity()`	≥ 1 events in $[a, b)$ from $\Lambda(t), \Lambda^{-1}(t)$
	`ztdraw_intensity()`	≥ 1 events in $[a, b)$ from $\lambda(t), \lambda_*(t)$
	`ztdraw_intensity_step()`	≥ 1 events in $[a, b)$ from $\lambda(t)$ and piecewise constant $\lambda_*(t)$
Time varying, general case, vectorized	`vdraw()`	(wrapper function)
	`vdraw_intensity_step_regular()`	≥ 0 events in $[a, b)$ from $\lambda(t)$ and piecewise constant $\lambda_*(t)$
	`vztdraw_intensity_step_regular()`	≥ 1 events in $[a, b)$ from $\lambda(t)$ and piecewise constant $\lambda_*(t)$
(Helper function)	`get_step_majorizer()`	(obtains piecewise constant $\lambda_*(t)$ from $\lambda(t)$)

The table pertains to version 0.1.4 of **nhppp**. $\lambda(t)$ is an intensity function, $\lambda_*(t)$ a majorizer function for $\lambda(t)$, $\Lambda(t)$ the integrated intensity function, and $\Lambda^{-1}(t)$ the inverse function (preimage) of $\Lambda(t)$.

the process is memoryless: For any time t_0, the behavior of the process is independent to what happened before that time.

2.2 Homogeneous Poisson point process and counting process

Assume that the next event after time t_0 happens at time $t_0 + X$. It follows from the above definition (see [18, par. 4.1]) that, for a constant λ, X is exponentially distributed

$$X \sim \text{Exponential}(\lambda), \tag{2}$$

and that the number of events is Poisson distributed over the compact interval $(a, b]$, i.e.,

$$N(a, b) \sim \text{Poisson}(\lambda(b - a)). \tag{3}$$

Equation (2) generates the homogeneous Poisson point process $Z_1 = t_0 + X_1, Z_2 = Z_1 + X_2, \ldots$, where Z_i is the time of arrival of event i and X_i the inter-arrival times. We will use $Z_{(j)}$ to denote the event in position j when events are ordered in increasing time. Equation (3) describes the corresponding (dual) counting process $N_1 = N(t_0, Z_1), N_2 = N(t_0, Z_2), \ldots$, where N_i is the total number of events from time t_0 to time Z_i. The point process (the sequence $[Z_i]$ of event times) and the counting process (the sequence $[N_i]$ of cumulants) are two sides of the same coin.

Sampling from the constant rate point process in (2) is discussed in Section 3.

2.3 Non homogeneous Poisson point process and counting process

When the intensity function changes over time, the homogeneous Poisson point process generalizes to its non-stationary counterpart, an NHPPP, with intensity function $\lambda(t) > 0$. For details see reference [18, par 4.2]. Then, the number of events over the interval $(a, b]$ becomes

$$N(a, b) \sim \text{Poisson}(\Lambda(a, b)), \tag{4}$$

where $\Lambda(a, b) = \int_a^b \lambda(t)\, dt$ is the integrated intensity or cumulative intensity of the NHPPP. Equation (4) describes the counting process of the NHPPP, which in turn implies a stochastic point process – a distribution of events over time.

Here the simulation task is to sample event times from the point process that corresponds to intensity function $\lambda(t)$, or equivalently, to the integrated intensity

function $\Lambda(t) = \int_0^t \lambda(s)\ ds$ (Section 4). (With some abuse of notation, we define $\Lambda(t) \coloneqq \Lambda(0, t)$ when $a = 0$.)

2.3.1 A note on zero intensity processes

In (1), λ is strictly positive but in **nhppp** we allow it to be non-negative. If $\lambda = 0$, $\Pr[N(t, t + \Delta t) = 0] = 1$ and $\Pr[N(t, t + \Delta t) \geq 1] = 0$. This means that no events occur and the stochastic point process in the interval $(t, t + \Delta t]$ is denegerate. Allowing $\lambda(t) \geq 0$ has no bearing on the results of simulations. If

$$\lambda(t) \begin{cases} > 0, \text{ for } t \in (a, b] \\ = 0, \text{ for } t \in (b, c] \\ > 0, \text{ for } t \in (c, d] \end{cases}$$

we can always ignore the middle interval in which no events happen.

2.4 Properties that are important for simulation

2.4.1 Composability and decomposability of NHPPPs

The definition (1) implies that NHPPPs are composable [18, par. 4.2]: merging two NHPPPs with intensity functions $\lambda_1(t), \lambda_2(t)$ yields a new NHPPP with intensity function $\lambda(t) = \lambda_1(t) + \lambda_2(t)$. The reciprocal is also true: one can decompose an NHPPP with intensity function $\lambda(t)$ into two NHPPPs, one with intensity function $\lambda_1(t) < \lambda(t)$ and one with intensity function $\lambda_2(t) = \lambda(t) - \lambda_1(t)$. An induction argument extends the above to merging and decomposing three or more processes.

The composability and decomposability properties are important for simulation because they

- give the flexibility to simulate several parallel NHPPPs independently versus to merge them, simulate from the merged process, and then attribute the realized events to the component processes by assigning the i-th event to the j-th process with probability $\lambda_j(Z_i)/\lambda(Z_i)$, where $\lambda(t) = \sum \lambda_j(t)$.
- motivate a general sampling algorithm (Algorithm 4, "thinning" [19]) that simulates a target NHPPP with intensity $\lambda_1(t)$ by first drawing events from an

easy-to-sample NHPPP with intensity $\lambda(t) > \lambda_1(t)$, and then accepts sample i with probability $\lambda_1(Z_i)/\lambda(Z_i)$.

2.4.2 Transformations of the time axis

Strictly monotonic transformations of the carrier space of an NHPPP yield an NHPPP [20]. Consider an NHPPP with intensity functions $\lambda(t)$ and a strictly monotonic transformation of the time axis $u : t \mapsto \tau$ that is differentiable once almost everywhere. On the transformed time axis the point process is an NHPPP with intensity function

$$\rho(\tau) = \lambda(\tau) \left(\frac{du}{dt} \right)^{-1}. \tag{5}$$

This property is important for simulation because

- it motivates the use of another general sampling algorithm (Algorithm 5, "time transformation" or "inversion", [20]): A smart choice for u yields an easy to sample point process. The event times in the original time scale can be obtained as $Z_i = u^{-1}(\zeta_i)$, where ζ_i is the i-th event in the transformed time axis and u^{-1} is the inverse function of u.
- given that at least i events have realized in the time interval $(a, b]$, it makes it possible to draw events $Z_{(j)}, j < i$ given event $Z_{(i)}$. This is useful for simulating earlier events conditional on the occurrence of a subsequent event. Choosing $u(t) := Z_{(i)} - t$ makes the time count backwards from $Z_{(i)}$. In this reversed clock we draw as if in forward time exactly $i - 1$ events $\zeta_{(1)}, \zeta_{(2)}, \ldots, \zeta_{(i-1)}$. Back transforming yields all preceding events.

Table 2 summarizes the common simulation tasks, such as simulating single events (at most one, exactly one), a series of events (possibly demanding the occurrence of at least one event), or the occurrence of a prior (event $i - 1$ given $Z_{(i)}$). The **nhppp** package implements functions to simulate these tasks for general $\lambda(t)$ or $\Lambda(t)$.

3 Sampling the constant rate Poisson process

Sampling the constant rate Poisson process is straightforward. Algorithms 1 and 2 are two ways to sample event times in interval $(a, b]$ with constant intensity λ. Algorithm 3

Table 2. Common simulation needs in discrete event simulation.

#	Sampling task	Sampled times	Number of sampled events	Example
I	Any next event	$\{\}$ or $\{Z_{(1)}\}$	0 or 1	Single event that may (or may not) occur in the interval: death, progression from Stage I to Stage II cancer.
II	Exactly one next event	$\{Z_{(1)}\}$	1	Single event which must occur in the interval: death from any cause in a lifetime-horizon simulation.
III	Any and all events	$\{\}$ or $\{Z_{(1)}, Z_{(2)}, \dots\}$	≥ 0	Zero, one, or more events: emergence of one or more bladder tumors.
IV	At least one next event	$\{Z_{(1)}, Z_{(2)}, \dots\}$	≥ 1	One or more events: emergence of bladder tumors when simulating only patients with bladder tumors.
V	Event $i-1$ given $Z_{(i)}$	$\{Z_{(i-1)}\}$	1	Find the previous event when simulating conditional on a future event: time of symptom onset given the time of symptom-driven diagnosis; onset of Stage I cancer given progression from Stage I to Stage II cancer.

All listed tasks involve sampling events over the interval $(a, b]$ with known $\lambda(t)$ or $\Lambda(t)$.

describes sampling event times conditional on observing at least k events within the interval of interest.

3.1 Sequential sampling

Algorithm 1 samples events sequentially, using the fact that the inter-event times X_i are exponentially distributed with mean λ^{-1} [18, par. 4.1]. It involves generation only of exponential random variates, which is cheap on modern hardware. To sample at most k events, change the condition for the while loop in line 3 to

$$\textbf{while } t < b \ \& \ |\mathcal{Z}| < k \textbf{ do}.$$

The package's `ppp_sequential()` function implements constant-rate sequential sampling that returns a vector with zero or more event times in the interval $[a, b)$. The `range_t` argument is a two-values vector with the bounds a, b. Setting the optional argument `atmost1` to `TRUE` from its default value of `FALSE` returns the first event or an empty vector, depending on whether at least one event is drawn in the interval.

Algorithm 1 Sequential sampling of events in interval $(a, b]$ with constant intensity λ.

Require: $t \in (a, b]$
$t \leftarrow a$
$\mathcal{Z} \leftarrow \emptyset$ ▷ $\mathcal{Z}$ is an ordered set
while $t < b$ **do** ▷ Up to k earliest points: **while** $t < b$ & $|\mathcal{Z}| < k$ **do**
  $X \leftarrow X \sim \text{Exponential}(\lambda^{-1})$ ▷ Mean-parameterized
  $t \leftarrow t + X$
  if $t < b$ **then**
    $\mathcal{Z} \leftarrow \mathcal{Z} \cup \{t\}$
  end if
end while
return $\mathcal{Z}$

```
R> library("nhppp")

R> ppp_sequential(range_t = c(7, 10), rate = 1, atmost1 = FALSE)

[1] 7.673885 8.650502 9.011229 9.407575
```

nhppp functions can accept a user provided random number stream object via the `rng_stream` option.

```
R> library("rstream")

R> S <- new("rstream.mrg32k3a")

R> ppp_sequential(range_t = c(7, 10), rate = 1, rng_stream = S)

[1] 8.793702
```

3.2 Sampling using order statistics

Algorithm 2 Sampling events in interval $(a, b]$ with constant intensity λ using order statistics.

Require: $t \in (a, b]$
$N \leftarrow N \sim \text{Poisson}\big(\lambda(b - a)\big)$
$t \leftarrow a$
$\mathcal{Z} \leftarrow \emptyset$ ▷ $\mathcal{Z}$ is an ordered set
if N > 0 **then**
  for $i \in [N]$ **do**:
    $U_i \leftarrow U_i \sim \text{Uniform}(0, 1)$ ▷ Generate order statistics
    $\mathcal{Z} \leftarrow \mathcal{Z} \cup \{a + (b - a)U_i\}$
  end for
  $\mathcal{Z} \leftarrow \text{sort}(\mathcal{Z})$
end if
return $\mathcal{Z}$ ▷ Up to k earliest points: **return** $\{Z_{(i)} \mid i \leq k\ , Z_{(i)} \in \mathcal{Z}\}$

Algorithm 2 first draws the number of events in $(a, b]$ from a Poisson distribution. Conditional on the number of events, the event times Z_i are uniformly distributed over $(a, b]$ [18, par. 4.1]. The algorithm returns the order statistics $[Z_{(i)}]$, obtained by sorting the event times $[Z_i]$ in ascending order. It is necessary to generate all event times to generate the order statistics. Thus, to sample at most k event times we should return the earliest k event times, and line 11 of the Algorithm would be changed to

$$\textbf{return } \{Z_{(i)} \mid i \leq k, Z_{(i)} \in \mathcal{Z}\}.$$

The `ppp_orderstat()` function implements constant-rate sampling via the order-statistics algorithm.

```
R> ppp_orderstat(range_t = c(3.14, 6.28), rate = 1/2)
```

```
[1] 3.141663 5.700931
```

3.3 Sampling conditional on observing at least m events

Algorithm 3 Sampling with constant intensity λ conditional that at least m events occurred in interval $(a, b]$. Relies on generating order statistics analogously to Algorithm 2.

Require: $t \in (a, b]$
1: $N \leftarrow N \sim \text{TruncatedPoisson}_{N \geq m}\big(\lambda(b-a)\big)$ ▷ $(m-1)$-truncated Poisson
2: $t \leftarrow a$
3: $\mathcal{Z} \leftarrow \emptyset$ ▷ $\mathcal{Z}$ is an ordered set
4: **if** N > 0 **then**
5: **for** $i \in [N]$ **do**:
6: $U_i \leftarrow U_i \sim \text{Uniform}(0, 1)$ ▷ Generate order statistics
7: $\mathcal{Z} \leftarrow \mathcal{Z} \cup \{a + (b-a)U_i\}$
8: **end for**
9: $\mathcal{Z} \leftarrow \text{sort}(\mathcal{Z})$
10: **end if**
11: **return** $\mathcal{Z}$ ▷ Up to k earliest points: **return** $\{Z_{(i)} \mid i \leq k\ , Z_{(i)} \in \mathcal{Z}\}$

Algorithm 3 is used to generate a point process conditional on observing at least m events. For example, if λ is the intensity of tumor generation, it can be used to simulate times of tumor emergence among patients with at least one ($m = 1$) tumor. To return the up to k earliest events, we modify line 11 the same way as for Algorithm 2. As an example, in a lifetime simulation we can sample the time of all-cause death by setting in Algorithm 3 $m = 1$, so that at least one event will happen in $(a, b]$, and $k = 1$, to sample only the time of the first event $Z_{(1)}$.

To sample exactly m events, change line 1 of Algorithm 3 to

$$N \leftarrow m.$$

Function `ztppp()` simulates times conditional on drawing at least one event - i.e., setting $m = 1$ in Algorithm 3 to sample from a zero truncated Poisson distribution in line 1.

```
R> ztppp(range_t = c(0, 10), rate = 0.001, atmost1 = FALSE)

[1] 4.411277
```

Function `ppp_n()` simulates times conditional on drawing exactly m events.

```
R> ppp_n(size = 4, range_t = c(0, 10))

[1] 1.762014 2.902897 6.751627 9.733794
```

4 The general sampling algorithms used in nhppp

The **nhppp** package uses three well known general sampling algorithms, namely thinning, time transformation or inversion, and order-statistics. These algorithms are efficiently combined to sample from special cases, including cases where the intensity function is a piecewise constant, linear, or log-linear function of time, as described in Section 5.2.

The thinning algorithm works with the intensity function $\lambda(t)$, which is commonly available. The inversion and order statistics algorithms have smaller computational cost than the thinning algorithm, but work with the integrated intensity function $\Lambda(t)$ and its inverse $\Lambda^{-1}(z)$, which may not be available. The generic function `draw()` is a wrapper function that dispatches to specialized functions depending on the provided arguments. It is useful for general tasks but the specialized functions are probably faster.

```
R> l <- function(t) t
R> L <- function(t) 0.5 * t^2
R> Li <- function(z) sqrt(2 * z)
R> draw(
+    lambda = l, lambda_maj = l(10), range_t = c(5, 10),
```

```
+    atmost1 = FALSE, atleast1 = FALSE
+  ) |> head(n = 5)

[1] 5.179473 5.374814 5.957391 5.992196 6.101935

R> draw(
+    Lambda = L, Lambda_inv = Li, range_t = c(5, 10),
+    atmost1 = FALSE, atleast1 = FALSE
+  ) |> head(n = 5)

[1] 5.219264 5.230747 5.369646 5.398531 5.618079
```

4.1 The thinning algorithm

The thinning algorithm relies on the decomposability of NHPPPs (Section 2.4) and is described in [19]. Let the target NHPPP have intensity function $\lambda(t)$ and $\lambda_*(t) \geq \lambda(t)$ for all $t \in (a, b]$ be a majorizing intensity function. Think of the majorizing function as an easy-to-sample function which is the sum of the intensity of the target point process $\lambda(t)$ and the intensity $\lambda_{reject}(t)$ of its complementary point-process,

$$\lambda_*(t) = \lambda(t) + \lambda_{reject}(t).$$

The acceptance-rejection scheme in Algorithm 4 generates proposal samples with intensity function $\lambda_*(t)$ and stochastically attributes them to the target process (to keep, with probability $\lambda(Z)/\lambda_*(Z)$) or its complement.

To sample the earliest k points, one can exit the for loop in lines 4-9 when k events have been sampled in line 7, or, alternatively, return the first up to k points in line 11.

A measure of the efficiency of Algorithm 4 is the proportion of samples that are accepted, which is

$$\frac{\int_a^b \lambda(t)\ \mathrm{d}t}{\int_a^b \lambda_*(t)\ \mathrm{d}t} \tag{6}$$

on average. Thus, the closer $\lambda_*(t)$ is to $\lambda(t)$, the more efficient the algorithm.

In practice, $\lambda_*(t)$ can be chosen as one of the special cases in Section 5, for which we have fast sampling algorithms. For example, it can be a piecewise constant majorizer. Algorithm A in S1 Appendix can automatically generate a piecewise constant majorizer

Algorithm 4 The thinning algorithm for sampling from $\lambda(t)$.

Require:

$\lambda_*(t) \geq \lambda(t)\ \forall\ t \in (a,])$ ▷ majorizing intensity function

$\mathcal{Z}_* = \{Z_i^* \mid Z_i^* \text{ are samples from } \lambda_*(t)\}$ ▷ $\mathcal{Z}_*$ is an ordered set

$N \leftarrow |\mathcal{Z}_*|$

$\mathcal{Z} \leftarrow \emptyset$ ▷ $\mathcal{Z}$ is an ordered set

if $N > 0$ **then**

  for $i \in [N]$ **do**:

    $U_i \leftarrow U_i \sim \text{Uniform}(0, 1)$

    if $U_i < \lambda(Z_{(i)}^*)/\lambda_*(Z_{(i)}^*)$ **then**

      $\mathcal{Z} \leftarrow \mathcal{Z} \cup \{Z_{(i)}^*\}$

    end if

  end for

end if

return $\mathcal{Z}$ ▷ Up to k earliest points: **return** $\{Z_{(i)} \mid i \leq k\ , Z_{(i)} \in \mathcal{Z}\}$

function for intensity functions that are monotonic and possibly non-continuous or Lipschitz continuous and possibly non-monotonic.

The **nhppp** package has functions that sample from time-varying intensity functions. The first function, `draw_intensity()`, expects a user-provided linear ($\lambda_*(t) = \alpha + \beta t$) or log-linear ($\lambda_*(t) = e^{\alpha+\beta t}$) majorizer function.

```
R> lambda_fun <- function(t) exp(0.02 * t)
R> draw_intensity(
+    lambda = lambda_fun, # linear majorizer
+    lambda_maj = c(intercept = 1.01, slope = 0.03),
+    exp_maj = FALSE, range_t = c(0, 10)
+  ) |> head (n = 5)

[1] 1.310245 2.094217 2.908682 3.268384 8.007606

R> draw_intensity(
+    lambda = lambda_fun, # log-linear majorizer
+    lambda_maj = c(intercept = 0.01, slope = 0.03),
+    exp_maj = TRUE, range_t = c(0, 10)
+  ) |> head (n = 5)

[1] 0.3406743 0.6079479 0.8441584 2.6424551 3.3185387
```

The second function, `draw_intensity_step()`, expects a user-provided piecewise

linear majorizer

$$\lambda_*(t) = \begin{cases} \lambda_1 & \text{for } t \in [a_1, b_1) = [a, b_1), \\ \dots & \\ \lambda_m & \text{for } t \in [a_m, b_m) \text{ with } a_m = b_{m-1}, \\ \dots & \\ \lambda_M & \text{for } t \in [a_M, b_M) = [a_M, b), \end{cases}$$

which is specified as a vector of length $M + 1$ including the points $(a, [b_m]_{m=1}^M)$ and a vector of length M with the values $[\lambda_m]_{m=1}^M$ in each subinterval of $(a, b]$. For example, the following code splits the interval $(0, 10]$ into $M = 10$ subintervals of length one. Because `lambda_fun()` is strictly increasing, its value at the upper bound of each subinterval is the supremum of the interval.

```
R> draw_intensity_step(
+    lambda = lambda_fun,
+    lambda_maj_vector = lambda_fun(1:10), # 1:10 (10 intensity values)
+    times_vector = 0:10 # 0:10 (11 interval bounds)
+  ) |> head(n = 5)
```

```
[1] 0.3825378 7.0822941 7.7839779 8.7766992 8.9554954
```

4.2 The time transformation or inversion algorithm

Algorithm 5 implements the time transformation or inversion algorithm from [20] and [18, par. 4.2]. As mentioned in Section 2.4, strictly monotonic transformations of the carrier space (here, time) of a Poisson point process yield another Poisson Point Process. In equation (5), choosing the transformation $\tau = u(t) = \Lambda(t)$, so that $\frac{du(t)}{dt} = \lambda(t)$, results in $\rho(\tau) = 1$.

This means (proof sketched in [18, par. 4.2]) that we can sample points from a Poisson point process with intensity one over the interval $(\tau_a, \tau_b] = (\Lambda(a), \Lambda(b)]$. Via a similar argument, we transform event times sampled on the transformed scale back to the original scale using $g(t) = \Lambda^{-1}(\tau)$. The transformations $u(\cdot), g(\cdot)$ are not unique – at least up to the group of affine transformations.

Function `draw_cumulative_intensity_inversion()` works with a cumulative intensity function $\Lambda(t)$ and its inverse $\Lambda^{-1}(z)$, if available. If the inverse function is not available (argument `Lambda_inv = NULL`), the Brent bisection algorithm is used to invert $\Lambda(t)$ numerically, at a performance cost [21].

```
R> Lambda_fun <- function(t) 50 * exp(0.02 * t) - 50
R> Lambda_inv_fun <- function(z) 50 * log((z + 50) / 50)
R> draw_cumulative_intensity_inversion(
+    Lambda = Lambda_fun,
+    Lambda_inv = Lambda_inv_fun,
+    range_t = c(5, 10.5),
+    range_L = Lambda_fun(c(5, 10.5))
+  ) |> head(n = 5)

[1]  6.458937  7.608496  9.060817  9.566278 10.076889
```

Algorithm 5 The time transformation or inversion algorithm for sampling given $\Lambda(t), \Lambda^{-1}(z)$ [18, 20]. The notation PoissonProcess_1 indicates sampling event times from a constant rate one Poisson point process.

Require: $\Lambda(t), \Lambda^{-1}(z), t \in (a, b]$ ▷ $\Lambda^{-1}(z)$ possibly numerically
1: $\tau_a \leftarrow \Lambda(a), \tau_b \leftarrow \Lambda(b)$
2: $\mathcal{C} \leftarrow \mathcal{C} \sim \text{PoissonProcess}_1(\tau_a, \tau_b)$ ▷ From Algorithm 1 (or 3 for conditional sampling)
3: $\mathcal{Z} \leftarrow \Lambda^{-1}(\mathcal{C})$ ▷ $\Lambda^{-1}(\cdot)$ as set function, meant elementwise
4: **return** $\mathcal{Z}$

4.3 The order statistics algorithm

The general order statistics algorithm (Algorithm 6) is a direct generalization of Algorithm 2. It first draws the number N of realized events. Conditional on N

$$\begin{aligned} U_{(i)} &= \frac{\Lambda(Z_{(i)}) - \Lambda(a)}{\Lambda(b) - \Lambda(a)} \sim \text{Uniform}(0, 1), \\ Z_{(i)} &= \Lambda^{-1}\Big(\Lambda(a) + U_{(i)}\big(\Lambda(b) - \Lambda(a)\big)\Big), \end{aligned} \tag{7}$$

as discussed in [19]. Algorithm 6 makes the above explicit.

Sampling up to k earliest points means returning the up to k earliest event times. If $\Lambda(t)$ is a positive linear function of time, λ is constant and Algorithm 6 becomes Algorithm 2.

Algorithm 6 The order statistics algorithm for sampling from an NHPPP given $\Lambda(t), \Lambda^{-1}(z)$.

Require: $\Lambda(t), \Lambda^{-1}(z), t \in (a, b]$ ▷ $\Lambda^{-1}(z)$ possibly numerically
$N \leftarrow N \sim \text{Poisson}\big(\Lambda(b) - \Lambda(a)\big)$
$t \leftarrow a$
$\mathcal{Z} \leftarrow \emptyset$ ▷ $\mathcal{Z}$ is an ordered set
if N > 0 **then**
  for $i \in [N]$ **do**:
    $U_i \leftarrow U_i \sim \text{Uniform}(0, 1)$ ▷ Generate order statistics
    $\mathcal{Z} \leftarrow \mathcal{Z} \cup \{\Lambda^{-1}\Big(\Lambda(a) + U_i\big(\Lambda(b) - \Lambda(a)\big)\Big)\}$
  end for
  $\mathcal{Z} \leftarrow \text{sort}(\mathcal{Z})$
end if
return $\mathcal{Z}$ ▷ Up to k earliest points: **return** $\{Z_{(i)} \mid i \leq k\ , Z_{(i)} \in \mathcal{Z}\}$

To sample conditional on observing at least m events in the interval $(a, b]$ see Algorithm B in S2 Appendix.

$$N \leftarrow N \sim \text{TruncatedPoisson}_{N \geq m}\big(\Lambda(b) - \Lambda(a)\big).$$

Function `draw_cumulative_intensity_orderstats()` works with a cumulative intensity function $\Lambda(t)$ and its inverse $\Lambda^{-1}(z)$, if available. Function `ztdraw_cumulative_intensity()` conditions that at least one event is sampled in the interval. As above, if the inverse function is not available (argument `Lambda_inv = NULL`), the Brent bisection algorithm is used to invert $\Lambda(t)$ numerically, at a performance cost.

```
R> draw_cumulative_intensity_orderstats(
+    Lambda = Lambda_fun,
+    Lambda_inv = Lambda_inv_fun,
+    range_t = c(4.1, 7.6)
+  )

[1] 5.091581 5.526070 5.601576 5.762498 6.495684

R> ztdraw_cumulative_intensity(
+    Lambda = Lambda_fun,
+    Lambda_inv = Lambda_inv_fun,
+    range_t = c(4.1, 7.6)
+  )
```

```
[1] 5.063676 6.682454 6.749162 6.926164 7.298342
```

5 Special cases

The **nhppp** package implements several special cases where the intensity function $\lambda(\cdot)$, the integrated intensity function $\Lambda(\cdot)$, and its inverse $\Lambda^{-1}(\cdot)$ have straightforward analytical expressions.

5.1 Sampling a piecewise constant NHPPP

Functions `draw_sc_step()` and `draw_sc_step_regular()` sample piecewise constant intensity functions based on Algorithm 5. The first can work with unequal-length subintervals $(a_m, b_m]$. The second results in a small computational time improvement when all subintervals are of equal length.

```
R> draw_sc_step(
+    lambda_vector = 1:5, times_vector = c(0.5, 1, 2.4, 3.1, 4.9, 5.9),
+    atmost1 = FALSE, atleast1 = FALSE
+  ) |> head(n = 5)

[1] 0.8425117 1.3281115 2.3309443 2.6794560 2.7939130

R> draw_sc_step_regular(
+    lambda_vector = 1:5, range_t = c(0.5, 5.9), atmost1 = FALSE,
+    atleast1 = FALSE
+  ) |> head(n = 5)

[1] 2.058468 2.100620 2.508954 3.125179 3.604882
```

Function `vdraw_sc_step_regular()` is a vectorized version of `draw_sc_step_regular()`. It returns a matrix with one event series per row, and as many columns as the maximum number of events across all draws.

```
R> vdraw_sc_step_regular(
+    lambda_matrix = matrix(runif(20), ncol = 5), range_t = c(1, 4),
+    atmost1 = FALSE
+  )

         [,1]     [,2]     [,3]     [,4]
[1,] 2.304123 2.802767       NA       NA
```

```
[2,] 2.990953       NA       NA       NA
[3,] 1.840374 2.134357 3.784424 3.816034
[4,] 2.136138 2.703826 3.269631       NA
```

The corresponding functions that return at least one event in the interval are `ztdraw_sc_step()`, `ztdraw_sc_step_regular()`, and `vztdraw_sc_step_regular()`.

5.2 Sampling NHPPPs with linear and log-linear intensities

Functions `draw_sc_linear()` and `ztdraw_sc_linear()` sample zero or more and at least one event, respectively, from NHPPPs with linear intensity functions. An optional argument (`atmost1`) returns the first event only.

$$\lambda(t) = \begin{cases} \alpha + \beta t & \text{for } t \in [a, b), t > -\frac{\alpha}{\beta} \\ 0 & \text{otherwise} \end{cases}.$$

```
R> draw_sc_linear(alpha = 3, beta = -0.5, range_t = c(0, 10)) |> head(n = 5)
```

```
[1] 0.3327657 0.4270154 0.5804320 0.6935027 0.9832093
```

```
R> ztdraw_sc_linear(alpha = 0.5, beta = 0.2, range_t = c(9.999, 10))
```

```
[1] 9.999757
```

An analogous set of functions (`[nhppp|ztnhppp]_sc_loglinear()`) samples from log-linear intensity functions

$$\lambda(t) = \begin{cases} e^{\alpha+\beta t} & \text{for } t \in [a, b) \\ 0 & \text{otherwise} \end{cases}.$$

The sampling algorithm is a variation of Algorithm 5, as described in [22]. Example usage follows.

```
R> draw_sc_loglinear(alpha = 1, beta = -0.02, range_t = c(8, 10))
```

```
 [1] 8.028806 8.128887 8.457669 8.483558 8.498647 8.503109 8.522725
 [8] 8.665979 8.671737 8.978065 8.981105 9.493691 9.815000 9.909167
```

```
R> ztdraw_sc_loglinear(alpha = 1, beta = -0.02, range_t = c(9, 10))

[1] 9.038160 9.075722 9.238302
```

6 Comparisons with other R packages

Table 3 lists five R packages that simulate from NHPPPs, including **nhppp**. We did not consider research code that is not an R package in the Comprehensive R Archive Network or is developed in other languages. For example, we do not run comparisons with the R and Python code for sampling from piecewise constant NHPPPs with regular time intervals in Garibay *et al* [23]. (Their code corresponds to the `vdraw_sc_step_regular()` function in **nhppp**.)

Package **reda** [24] focuses on recurrent event data analysis and can simulate NHPPPs with the inversion and thinning algorithms using the `simEvent()` function. It can take function object arguments for $\lambda(t)$. When using the thinning algorithm, it takes a constant majorizer. For the inversion algorithm, it approximates $\Lambda(t)$ and its inverse numerically, at a computational cost.

Package **simEd** [25] includes various functions for simulation education. Function `thinning()` implements the homonymous algorithm for drawing points from an NHPPP. Users can specify the intensity function and a piecewise constant or linear majorizer function.

Package **IndTestPP** [26] provides a framework for exploring the dependence between two or more realizations of point processes. It includes the ancillary function `simNHPc()` for simulating NHPPPs with the inversion or thinning algorithms. The function's argument is a piecewise constant approximation of the intensity function via a vector of evaluations, each corresponding to unit length subintervals. This resolution may not be adequate to simulate processes that change fast over a unit time interval.

Package **NHPoisson** [27, 28] fits NHPPP models to data and is not really geared towards mathematical simulation. Its `simNHP.fun()` function provides the ability for simulation-based inference via an implementation of the inversion algorithm. This function is designed to work with the package's inference machinery and is not practical to use for simulation, because the user has no direct control over the function's rescaling

of the time axis.

The claimed advantage of **nhppp** over the existing packages is that

- it samples from the target NHPPP and not from a numerical approximation thereof, e.g., as **IndTestPP** does.
- It can sample conditional on observing at least one event in the interval, which no other package implement.
- It accepts user-provided random number stream objects, which is useful for implementing simulation variance reduction techniques such as common random numbers [29] and antithetic variates [30].
- It is fast and memory efficient, both for the non-vectorized functions that are implemented in native `R` and for the vectorized functions that use `C++` plugins via the **Rcpp** package [31]. **nhppp** has specialized functions to leverage additional information about the point process, such as $\Lambda(t), \Lambda^{-1}(z)$, when available, which can result in faster simulation use the cumulative intensity function and its inverse, often at a computational speed advantage.

7 Illustrations

Depending on the application, we may have access to the intensity function or the integrated intensity function. We compared the `R` packages in Table 3 for sampling from a non-monotonic and highly non-linear intensity function for which the integrated intensity function can be derived analytically.

7.1 The target NHPPP to be simulated

Consider the example

$$\begin{aligned} \lambda(t) &= e^{rt}(1 + \sin wt), \\ \Lambda(t) &= \frac{e^{rt}(r \sin wt - w \cos wt) + w}{r^2 + w^2} + \frac{e^{rt} - 1}{r} \end{aligned} \tag{8}$$

of a sinusoidal intensity function $\lambda(t)$ scaled to have an exponential amplitude and one of its antiderivatives $\Lambda(t)$, with such a constant term that $\Lambda(0) = 0$. For the numerical

Table 3. NHPPP generation in `R` packages.

`R` package	Function	Algorithms (inputs)			Sample only earliest event	Custom RNG	Simulate given $N > 0$	Vectorized functions
		Thinning	Inversion	Order statistics				
nhppp	[see text]	$\lambda(t)$, $\lambda_*(t)$	$\Lambda(t), \Lambda^{-1}(z)$	$\Lambda(t), \Lambda^{-1}(z)$	Yes	**rstream** objects	Yes	For piecewise constant intensity
reda	`simEvent()`	$\lambda(t)$, λ_* constant	$\lambda(t)$ (no $\Lambda(t), \Lambda^{-1}(z)$)	No	Yes	No	No	No
simEd	`thinning()`	$\lambda(t)$, $[\lambda_{*m}]_{m=1}^{M}$	No	No	No	No	No	No
IndTestPP	`simNHPc()`	$[\lambda_m]_{m=1}^{M}$, λ_* constant	$[\lambda_m]_{m=1}^{M}$ (no $\Lambda(t), \Lambda^{-1}(z)$)	No	No	No	No	No
NHPoisson	`simNHP.fun()`	No	$\lambda(t)$, (no $\Lambda(t), \Lambda^{-1}(z)$)	No	No	No	No	No

RNG: random number generator object.

Fig 1. The $\lambda(t)$ (left) and $\Lambda(t)$ used in the illustration.

Also shown three majorizing functions (left panel, marked a, b, c) that are used with the thinning algorithm in the analyses.

study we set $r = 0.2$, $w = 1$, and $t \in (0, 6\pi]$. There is no analytic inverse function for this example. However, we can precompute `Li()`, a good numerical approximation to $\Lambda^{-1}(z)$. We will use it in Section 7.5 to compare the time performance of functions that use the inversion and order statistics algorithms when Λ^{-1} is available versus not.

```
R> l <- function(t) (1 + sin(t)) * exp(0.2 * t)
R> L <- function(t) {
+    exp(0.2 * t) * (0.2 * sin(t) - cos(t)) / 1.04 +
+      exp(0.2 * t) / 0.2 - 4.038462
+  }
R> Li <- approxfun(
+    x = L(seq(0, 6 * pi, 10^-3)),
+    y = seq(0, 6 * pi, 10^-3), rule = 2
+  )
```

Fig 1 graphs the intensity function and three majorizing functions over the interval of interest, which will be needed for the thinning algorithm.

The first, $\lambda_{*a}(t) = 43.38$, shown as a dashed blue line, is is a constant majorizer equal to the maximum of the intensity function. A constant majorizer may be a practical choice when only an upper bound is known for $\lambda(t)$. From (6), the analytic efficiency of the thinning algorithm using this majorizer is 0.209.

The second, $\lambda_{*b}(t)$, shown as a thin black line, is a piecewise constant envelope generated automatically from Algorithm A (in S1 Appendix) with 20 equal-length subintervals and Lipschitz cone coefficient $K = 52.05$. We set K equal to the maximum value of $|\frac{d\lambda(t)}{dt}|$ in the interval, attained at 6π. The analytic efficiency of the thinning algorithm using this majorizer is 0.245.

The third, $\lambda_{*c}(t)$, shown as a thicker black line, is a tighter piecewise constant majorizer with the same 20 equal-length subintervals that is constructed by finding a least upper bound in each subinterval. The analytic efficiency of the thinning algorithm

with the third majorizer is 0.718.

7.2 Simulation functions and algorithms

We sampled series of events from the target NHPPP using the packages and functions listed in Table 3. We repeated the sampling 10^4 times, recording all simulated points (event times). We also recorded the median computation time for drawing one series of events with single-threaded computation on modern hardware.

From the **nhppp** package we use

1. two functions that take as argument the intensity function and are based on Algorithm 4 (thinning): `draw_intensity()`, which uses linear majorizers such as λ_{*a}, and `draw_intensity_step()`, which uses piecewise constant majorizers such as λ_{*b} and λ_{*c} in the example.

2. Function `draw_cumulative_intensity_inversion()`, which takes as argument the cumulative intensity function $\Lambda(t)$ and is based on Algorithm 5 (time transformation/inversion), and

3. function `draw_cumulative_intensity_orderstats()`, which also uses $\Lambda(t)$ and is based on Algorithm 6 (order statistics).

Regarding the other `R` packages in Table 3, we used all except for **NHPoisson**, whose simulation function is tailored to supporting simulation based inference for data analysis and is not practical to use as a standalone function. (Its implementation does not allow the user to control the scaling of the time axis in a practical way.) However, its source code/algorithm is very similar to that of the **IndTestPP** simulation function, which is developed by the same authors.

We used the metrics in Table 4 to assess simulation performance with each function. We compared the empirical versus the simulated distributions of number of events and event times over $J = 100$ simulation runs.

7.3 Simulation performance with respect to number of events

We calculated the absolute and relative bias in the first two moments of the empirical distribution in the counts of events, the bounds of equal-tailed confidence intervals at

Table 4. Simulation metrics for the number of counts.

Metric	Definition	Description
Bias in mean	$B_\mu = \frac{1}{J}\sum_j n_j - N$	Mean difference from target in the number of counts.
Relative bias in mean	$B_{\mu,rel} = \frac{B_\mu}{N}$	Mean proportional difference from target in the number of counts.
Bias in variance	$B_V = \frac{1}{J}\sum_j \left(n_j - \frac{1}{J}\sum_j n_j\right)^2 - V$	Mean difference from target in variance of counts.
Relative bias in variance	$B_{V,rel} = \frac{B_V}{V}$	Mean proportional difference from target in variance of counts.
Equal-tailed p% confidence interval bounds	$n_{[p/2]}, n_{[1-p/2]}$	Quantiles of the empirical distribution of counts.
Goodness of fit p value	Statistic $\sum_x \frac{(O_x - E_x)^2}{E_x} \sim \chi^2_{U-L+1}$	Left-tail p value. p values near 1 imply good fit.
Wasserstein-1 distance	W_1, the smallest rearrangement of probability mass so that one distribution matches the other.	$W_1 = 0$ implies good fit
p value for $W_1 \neq 0$	Asymptotic theory p value	Two-sided p value. p values near 1 imply good fit.

In the Table, $j \in [J]$ indexes simulations, n_j is the number of counts in simulation j, $N = \Lambda(6\pi) - \Lambda(0)$ is the theoretical mean number of counts, and $V = \Lambda(6\pi) - \Lambda(0) = N$ the theoretical variance. The lower and upper bounds of an equal-tailed p% confidence interval, $p \in \{95, 90, 75, 50\}$, are denoted with $n_{[p/2]}, n_{[1-p/2]}$, respectively. For the goodness of fit, we created bins $[0, L), [L, L+1), \ldots, [U, \infty)$, where L, U are the 0.001 and 0.999 percentiles of the Poisson distribution with parameter $\Lambda(6\pi) - \Lambda(0)$. We indexed bins with $x \in \{1, \ldots, U - L + 2\}$. The goodness of fit statistic contrasts the observed (O_x) versus expected (E_x) numbers of events over the bins and it is compared with a χ^2_{U-L+1} distribution to obtain a p value.

the 95, 90, 75, and 50 percent levels, a χ^2-distributed goodness of fit statistic and its p-value, and the Wasserstein-1 distance W_1 between the empirical and the theoretical count distributions and the asymptotic one sided p value to reject whether $W_1 = 0$ according to [32]. W_1 is the smallest mass that has to be redistributed so that one distribution matches the other. W_1 is equal to the unsigned area between the cumulative distribution functions of the compared distributions. For example, $W_1 = 5.25$ means that the mass that must be moved to transform one density to the other is no less than 5.25 counts and a $W_1 = 0$ implies perfect fit.

The results for the **nhppp** functions in Fig 2 and Table 5 suggest excellent simulation performance.

The respective results for the `R` packages are in Fig 3 and Table 6. The simulation performance with the **reda** functions is excellent. Performance with **simEd** and

Fig 2. Theoretical (red) and empirical (black) cumulative distribution functions for event counts in the illustration example with nhppp functions.

The unsigned area between the theoretical and empirical curves equals the Wasserstein-1 distance in Table 5.

Table 5. Simulated total number of events with nhppp functions for the illustration example.

	Thinning $\lambda_*=\lambda_{*a}$	Thinning $\lambda_*=\lambda_{*b}$	Thinning $\lambda_*=\lambda_{*c}$	Inversion	Order statistics
Sample mean	171.057	171.257	171.322	171.193	171.131
B_μ	-0.078	0.122	0.187	0.058	-0.004
$B_{\mu,rel}$	-0.045	0.071	0.109	0.034	-0.002
Sample variance	175.015	168.218	173.918	166.950	166.933
B_V	3.880	-2.917	2.783	-4.185	-4.201
$B_{V,rel}$	2.267	-1.704	1.626	-2.445	-2.455
Goodness of fit, χ^2 [p value]	0.145 [1.000]	0.160 [1.000]	0.117 [1.000]	0.384 [1.000]	0.229 [1.000]
W_1 [p value]	0.194 [1.000]	0.189 [1.000]	0.231 [0.997]	0.195 [1.000]	0.187 [1.000]
Equal tail 95% CI = [146, 197]	[146, 197]	[146, 197]	[146, 197]	[146, 197]	[146, 197]
Equal tail 90% CI = [150, 193]	[150, 193]	[150, 193]	[150, 193]	[150, 193]	[150, 193]
Equal tail 75% CI = [156, 186]	[156, 186]	[156, 186]	[156, 187]	[156, 186]	[156, 186]
Equal tail 50% CI = [162, 180]	[162, 180]	[162, 180]	[162, 180]	[162, 180]	[162, 180]

Equal tail p% CI: a confidence interval whose bounds are the $p/2$ and $(1-p/2)$ count percentiles of the respective cumulative distribution function.

IndTestPP functions depends on the adequacy with which they approximate the target density. In this example, the approximation accuracy is not ideal for either package, but is somewhat worse for **IndTestPP**.

Fig 3. Theoretical (red) and empirical (black) cumulative distribution functions for event counts in the illustration example with the `R` packages in Table 3.

The unsigned area between the theoretical and empirical curves equals the Wasserstein-1 distance in Table 5.

7.4 Event times

We compared the theoretical and empirical distribution of event times for all $J = 10^4$ event time draws. We calculated a goodness of fit statistic by binning realized times in 70 bins and its p value, by comparing the statistic against the χ^2_{69} distribution. We also calculated the W_1 distance between these distributions and its associated p value.

Fig 4 and Table 7 indicate excellent simulation performance with the **nhppp** functions.

Fig 5 and Table 8 indicate excellent simulation performance with the **reda** functions.

Table 6. Simulated total number of events with the R packages of Table 3 for the illustration example.

	reda thinning, $\lambda_*=\lambda_{*a}$	**reda** inversion	**simEd** thinning, $\lambda_*=\lambda_{*a}$	**IndTestPP** thinning, no λ_*	**IndTestPP** inversion
Sample mean	172.430	174.170	179.910	190.490	191.030
B_μ	1.295	3.035	8.775	19.355	19.895
$B_{\mu,rel}$	0.757	1.774	5.128	11.310	11.626
Sample variance	168.429	145.193	155.355	194.838	191.484
B_V	-2.705	-25.942	-15.779	23.704	20.349
$B_{V,rel}$	-1.581	-15.159	-9.220	13.851	11.891
Goodness of fit, χ^2 [p value]	6.830 [1.000]	10.720 [1.000]	67.482 [0.994]	226.107 [<0.001]	237.199 [<0.001]
W_1 [p value]	1.453 [0.256]	3.083 [0.112]	8.856 [<0.001]	19.356 [0.086]	19.896 [0.170]
Equal tail 95% CI = [146, 197]	[152, 199]	[152, 196]	[161, 203]	[163, 214]	[168, 217]
Equal tail 90% CI = [150, 193]	[154, 195]	[154, 192]	[161, 203]	[167, 214]	[170, 215]
Equal tail 75% CI = [156, 186]	[158, 189]	[161, 187]	[169, 202]	[174, 205]	[176, 207]
Equal tail 50% CI = [162, 180]	[162, 181]	[165, 180]	[170, 183]	[178, 201]	[181, 200]

Equal tail p% CI: a confidence interval whose bounds are the $p/2$ and $(1-p/2)$ count percentiles of the respective cumulative distribution function.

Fig 4. Simulated event times with nhppp.

Left column: histogram (gray) and theoretical distribution (red) of event times; right column: empirical (black) and theoretical (red) cumulative distribution function. The unsigned area between the empirical and cumulative distribution functions is the W_1 distance in Table 7.

Table 7. Goodness of fit of simulated event times with nhppp functions for the example.

	Goodness of fit, χ^2 [p value]	W_1 [p value]
Thinning $\lambda_*=\lambda_{*a}$	0.004 [1.000]	0.396 [1.000]
Thinning $\lambda_*=\lambda_{*b}$	0.004 [1.000]	0.361 [1.000]
Thinning $\lambda_*=\lambda_{*c}$	0.004 [1.000]	0.338 [1.000]
Inversion	0.004 [1.000]	0.347 [1.000]
Order statistics	0.004 [1.000]	0.350 [1.000]

The simulation performance with the **simEd** and **IndTestPP** functions, which rely on approximations, is not as good.

Table 8. Goodness of fit of simulated event times with R functions in Table 3.

	Goodness of fit, χ^2 [p value]	W_1 [p value]
reda thinning ($\lambda_*=\lambda_{*a}$)	0.012 [1.000]	0.356 [1.000]
reda inversion	0.010 [1.000]	0.354 [1.000]
simEd thinning ($\lambda_*=\lambda_{*a}$)	0.028 [1.000]	0.338 [0.990]
IndTestPP thinning (no λ_*)	0.460 [1.000]	2.152 [0.930]
IndTestPP inversion	0.490 [1.000]	2.372 [0.927]

Fig 5. Simulated event times with the `R` packages in Table 3.

Left column: histogram (gray) and theoretical distribution (red) of event times; right column: empirical (black) and theoretical (red) cumulative distribution function. The unsigned area between the empirical and cumulative distribution functions is the W_1 distance in Table 8.

7.5 Time performance

7.5.1 Time performance of non-vectorized functions

To indicate time performance, we benchmarked functions by recording execution times when drawing a series of points (Fig 6). We also benchmarked functions for drawing the first-occurring event, because **nhppp** functions can sample the first time more efficiently when the inversion algorithm is used (Fig 7).

Fig 6. Computation times when drawing all events in interval.

Fig 7. Computation times when drawing the first event in interval.

We provided functions with the arguments they need to run fastest. For example, functions that use the inversion or order statistics algorithm execute faster when the inverse function $\Lambda^{-1}(z)$ is provided, rather than numerically calculated, as shown in both Figures for the **nhppp** package. (Functions in other packages do not take $\Lambda(t)$ and $\Lambda^{-1}(z)$ arguments.) The fastest functions are **nhppp** functions that rely on the inversion or order statistics algorithms given $\Lambda^{-1}(z)$.

According to (6), the thinning algorithm has higher efficiency, and is expected to execute faster, for majorizer functions that envelop the intensity function more closely. Observe that $\lambda_{*a} \succ \lambda_{*c}$ and $\lambda_{*b} \succ \lambda_{*c}$ in Fig 1. As expected, the execution times are indeed shorter for majorizer 'c' compared to 'b' in Figures 6 and 7. However, the execution times are longer with majorizer 'c' compared to 'a' because `draw_intensity()`, the function that uses constant majorizers, and `draw_intensity_step()`, the function that use piecewise constant majorizers, are implemented differently. `draw_intensity()` happens to be faster in this example, but this is not always true.

In **nhppp**, functions that use the inversion or order statistics algorithms can exit earlier when only the first event is requested. This is not possible, however, for the

thinning algorithm. This efficiency does not appear to be implemented in the other packages.

7.5.2 Time performance of vectorized functions

In `R`, 'vectorized' computation, where operations are done in columns, is faster than using `for` loops or `apply()` functions. As shown in Table 1, **nhppp** includes vectorized functions for sampling from (i) piecewise constant intensity functions, using `[vdraw|vztdraw]_sc_step_regular()`; and (ii) general intensity functions, using `[vdraw|vztdraw]_intensity_step_regular()`.

We compared the execution speed of non-vectorized and vectorized functions for sampling 10^5 times from the piecewise constant 'b' majorizer (λ_{*b}) in Fig 1. The expected number of events with λ_{*b} in $(0, 6\pi]$ is 741.97. When drawing only the earliest event, the vectorized function is approximately 113 times faster than the non-vectorized function (median $59ms$ versus $6717ms$ over 10^5 simulations). When drawing all events , the vectorized function is approximately 1.4 times faster than the non-vectorized function (median $36.55s$ versus $50.97s$ over 10^5 simulations). The reason that the difference in speed attenuates is that the current implementation of the vectorized functions does not use sparse matrices to store samples, which introduces inefficiencies the expected number of samples becomes larger.

8 Summary and next developments

The **nhppp** facilitates the simulation of NHPPPs from time-varying intensity or cumulative intensity functions. Its claim is that it (i) simulates correctly from a target density, not just from an approximation; (ii) samples conditional on observing at least one event in an interval; (iii) accomodates user provided random number stream objects; and (iv) is fast. The current version includes one vectorized function for sampling from regular-spaced piecewise constant intensity functions. In future releases we will further optimize execution speed and memory usage.

Computational details and credits

R 4.3.1 [33] was used for all analyses. Packages **xtable** 1.8.4 [34] and **knitr** 1.45 [35] were used for automatic report generation. Packages **ggplot2** 3.4.4 [36], **ggridges** 0.5.5 [37], and **latex2exp** 0.9.6 [38] were used for plot generation and LaTeXformatting. Packages **nhppp** 0.1.4 [16], **bench** 1.1.3 [39], **rstream** 1.3.7 [40], **otinference** 0.1.0 [41], and **parallel** 4.3.1 were used in the examples and the analyses.

All computations were done on an Apple M1 Max machine with 64 megabytes of random access memory. A preprint of the current paper is in [17]. R itself and all aforementioned packages are available from the Comprehensive R Archive Network (CRAN) at `https://CRAN.R-project.org/`.

Supporting information

S1 Appendix. Piecewise constant majorizer functions. Algorithm for the automatic generation of piecewise constant majorizer functions.

S2 Appendix. Conditional sampling from NHPPPs. Algorithm to sample conditionally on observing at least m events in $(a, b]$.

S3 R code. Code to reproduce the exhibits. R code to reproduce the exhibits. Timing results are machine and platform specific.

Acknowledgments

This work was funded from grant U01CA265750 from the National Cancer Institute. We thank the investigators of the Cancer Incidence and Surveillance Modeling Network (CISNET) Bladder Cancer Site Stavroula Chrysanthopoulou, Jonah Popp, Fernando Alarid-Escudero, Hawre Jalal, and David Garibay for useful discussions.

References

1. Law AM, Kelton WD, Kelton WD. Simulation modeling and analysis. vol. 3. Mcgraw-hill New York; 2007.

2. Luchak G. The solution of the single-channel queuing equations characterized by a time-dependent Poisson-distributed arrival rate and a general class of holding times. Operations Research. 1956;4(6):711–732.

3. Kim SH, Whitt W. Choosing arrival process models for service systems: Tests of a nonhomogeneous Poisson process. Naval Research Logistics (NRL). 2014;61(1):66–90.

4. Yang W, Su Q, Huang SH, Wang Q, Zhu Y, Zhou M. Simulation modeling and optimization for ambulance allocation considering spatiotemporal stochastic demand. Journal of Management Science and Engineering. 2019;4(4):252–265.

5. Zhou Z, Matteson DS, Woodard DB, Henderson SG, Micheas AC. A spatio-temporal point process model for ambulance demand. Journal of the American Statistical Association. 2015;110(509):6–15.

6. Abdel-Aty MA, Radwan AE. Modeling traffic accident occurrence and involvement. Accident Analysis & Prevention. 2000;32(5):633–642.

7. Thompson W. On the foundations of reliability. Technometrics. 1981;23(1):1–13.

8. England T, Harper P, Crosby T, Gartner D, Arruda EF, Foley K, et al. Modelling lung cancer diagnostic pathways using discrete event simulation. Journal of Simulation. 2023;17(1):94–104.

9. Rutter CM, Savarino JE. An evidence-based microsimulation model for colorectal cancer: validation and application. Cancer Epidemiol Biomarkers Prev. 2010;19(8):1992–2002. doi:10.1158/1055-9965.Epi-09-0954.

10. Jeon J, Meza R, Moolgavkar SH, Luebeck EG. Evaluation of screening strategies for pre-malignant lesions using a biomathematical approach. Math Biosci. 2008;213(1):56–70. doi:10.1016/j.mbs.2008.02.006.

11. Tsokos CP, Xu Y. Non-homogenous Poisson Process for Evaluating Stage I & II Ductal Breast Cancer Treatment. Journal of Modern Applied Statistical Methods. 2011;10(2):646–655. doi:10.22237/jmasm/1320121320.

12. Andreev VP, Head T, Johnson N, Deo SK, Daunert S, Goldschmidt-Clermont PJ. Discrete event simulation model of sudden cardiac death predicts high impact of preventive interventions. Scientific reports. 2013;3(1):1771.

13. Getsios D, Blume S, Ishak KJ, Maclaine GD. Cost effectiveness of donepezil in the treatment of mild to moderate Alzheimer's disease: a UK evaluation using discrete-event simulation. Pharmacoeconomics. 2010;28:411–427.

14. Mar J, Soto-Gordoa M, Arrospide A, Moreno-Izco F, Martínez-Lage P. Fitting the epidemiology and neuropathology of the early stages of Alzheimer's disease to prevent dementia. Alzheimer's research & therapy. 2015;7:1–8.

15. Zhang X. Application of discrete event simulation in health care: a systematic review. BMC health services research. 2018;18:1–11.

16. Trikalinos TA, Sereda Y. **nhppp**: Simulating Nonhomogeneous Poisson Point Processes in `R`; 2024. Available from: `https://CRAN.R-project.org/package=nhppp`.

17. Trikalinos TA, Sereda Y. **nhppp**: Simulating Nonhomogeneous Poisson Point Processes in `R`; 2024.

18. Cox D, Miller H. The Poisson Process. In: The Theory of Stochastic Processes. Chapman and Hall; 1965. p. 147.

19. Lewis PW, Shedler GS. Simulation of nonhomogeneous Poisson processes by thinning. Naval Research Logistics Quarterly. 1979;26(3):403–413.

20. Çinlar E. Introduction to stochastic processes Prentice-Hall. Englewood Cliffs, New Jersey (420p); 1975.

21. Press W, Teukolsky S, Vetterling W, Flannery B. Section 9.3. Van Wijngaarden-Dekker-Brent Method. Numerical Recipes: The Art of Scientific Computing. Cambridge University Press, New York; 2007.

22. Lewis P, Shedler G. Simulation of nonhomogeneous Poisson processes with log linear rate function. Biometrika. 1976;63(3):501–505.

23. Garibay D, Jalal H, Alarid-Escudero F. A computationally efficient nonparametric sampling (NPS) method of time to event for individual-level models. medRxiv. 2024;doi:10.1101/2024.04.05.24305356.

24. Wang W, Fu H, Yan J. **reda**: Recurrent Event Data Analysis; 2022. Available from: `https://github.com/wenjie2wang/reda`.

25. Lawson B, Leemis L, Kudlay V. **simEd**: Simulation Education; 2023. Available from: `https://CRAN.R-project.org/package=simEd`.

26. Cebrián AC. **IndTestPP**: Tests of Independence and Analysis of Dependence Between Point Processes in Time; 2020. Available from: `https://CRAN.R-project.org/package=IndTestPP`.

27. Cebrián AC, Abaurrea J, Asín J. **NHPoisson**: An `R` Package for Fitting and Validating Nonhomogeneous Poisson Processes. Journal of Statistical Software. 2015;64(6):1–25. doi:10.18637/jss.v064.i06.

28. Cebrián AC. **NHPoisson**: Modelling and Validation of Non-Homogeneous Poisson Processes; 2020. Available from: `https://CRAN.R-project.org/package=NHPoisson`.

29. Wright R, Ramsay Jr T. On the effectiveness of common random numbers. Management Science. 1979;25(7):649–656.

30. Hammersley JM, Mauldon JG. General principles of antithetic variates. In: Mathematical proceedings of the Cambridge philosophical society. vol. 52. Cambridge University Press; 1956. p. 476–481.

31. Eddelbuettel D, Francois R, Allaire J, Ushey K, Kou Q, Russell N, et al.. **Rcpp**: Seamless `R` and `C++` Integration; 2024. Available from: `https://CRAN.R-project.org/package=Rcpp`.

32. Sommerfeld M, Munk A. Inference for empirical Wasserstein distances on finite spaces. Journal of the Royal Statistical Society Series B: Statistical Methodology. 2018;80(1):219–238.

33. R Core Team. R: A Language and Environment for Statistical Computing; 2023. Available from: https://www.R-project.org/.

34. Dahl DB, Scott D, Roosen C, Magnusson A, Swinton J. **xtable**: Export Tables to LaTeXor HTML; 2019. Available from: https://CRAN.R-project.org/package=xtable.

35. Xie Y. **knitr**: A Comprehensive Tool for Reproducible Research in **R**. In: Stodden V, Leisch F, Peng RD, editors. Implementing Reproducible Computational Research. Chapman and Hall/CRC; 2014.

36. Wickham H. **ggplot2**: Elegant Graphics for Data Analysis. Springer-Verlag New York; 2016. Available from: https://ggplot2.tidyverse.org.

37. Wilke CO. **ggridges**: Ridgeline Plots in **ggplot2**; 2023. Available from: https://CRAN.R-project.org/package=ggridges.

38. Meschiari S. **latex2exp**: Use LaTeXExpressions in Plots; 2022. Available from: https://CRAN.R-project.org/package=latex2exp.

39. Hester J, Vaughan D. **bench**: High Precision Timing of R Expressions; 2023. Available from: https://CRAN.R-project.org/package=bench.

40. Leydold J. **rstream**: Streams of Random Numbers; 2022. Available from: https://CRAN.R-project.org/package=rstream.

41. Sommerfeld M. **otinference**: Inference for Optimal Transport; 2017. Available from: https://CRAN.R-project.org/package=otinference.

A. Reviewer 1 comments

R1.1: [No comments]

Reply: [No replies needed]

B. Reviewer 2 comments (R2)

R2.1: *The authors did not make any of the modifications we requested.*

Reply: The comments from Reviewer 2 in the first peer-review round were terse, unclear, and nonspecific. We cannot address comments that we do not understand. We have asked the Reviewer for clarifications to the original comments, or any additional comments, but have received none.

C. Reviewer 3 comments (R3)

R3.1: *The results of this paper are very useful in studies assuming a NHPPP* [sic] *modeling approach with different parametric intensity functions. In many situations, the statistical properties under a classical or a Bayesian approach are verified using simulated data assuming specified parametric intensity functions in NHPPP* [sic]. *This point should be discussed in the introduction section. Although, the importance of the study, the review of the literature on NHPPP* [sic] *should be improved as motivation for the use of the simulation codes (a software package in R) for different structures of NHPPP* [sic] *introduced in the paper.*

In my opinion, the paper could be published after improving the motivation for the need of simulated data assuming a NHPPP [sic] *modeling approach and the inclusion of new references on the use of NHPPP* [sic] *in the introduction section since the use of NHPPP* [sic] *in different applications (environment, epidemiology, economy, engineering) is becoming very popular as observed in the literature. Usually a NHPPP* [sic] *modeling approach is considered assuming different parametric intensity functions, sometimes in presence of one or more change-points, under a Bayesian approach given the difficulties to obtain accurate classical inferences (maximum likelihood estimates and related usual asymptotical results).*

In summary: it is needed to introduce a complete review of the literature on applications of NHPPP [sic] *(new references on the use of NHPPP* [sic] *in different areas) in the introduction section to have better motivation for the study.*

Reply: Following the reviewer's suggestion, we added a paragraph in the introduction to motivate the need for simulating from NHPPPs. It reads (reference numbers are omitted – see text):

"NHPPPs have been used in the simulation analysis of queues in queuing theory and operations research [ref]; hospital operations [ref]; ambulance services [ref]; traffic accidents [ref]; product and network reliability [ref]; and the modeling of cancer [ref], heart disease [ref], and dementia [ref], among other applications [ref]. NHPPPs are used so widely in part because their assumptions are often plausible. For example, when modeling traffic accidents along a road, it may be plausible to assume that individual accidents are independent of each other, but they happen in some locations more often because the probability of an accident depends on local aspects of the road, such as turns, slopes, and propensity for slippery conditions. Similarly, when modeling the impact of screening strategies on colorectal cancer outcomes at the population level, it is probably plausible to assume that, for each person, the emergence of precancerous lesions (adenomas) over a time interval is independent of whether such lesions emerged in other non-overlapping time intervals. In these examples, the intensity of event occurrence over the carrier space (the probability of a traffic accident along a road; and the probability that an adenoma will emerge in a person's colon at different ages) is captured by the NHPPP's intensity function. An NHPPP can model complicated event patterns using intensity functions that vary over the carrier space (e.g., length of road, time)."

D. Reviewer 4 comments (R4)

R4.1: *The proposed manuscript is good and has some merit, but it is not adequate for the* PLOS *journal. The authors should send it to* `R` Journal*, since it shows the performance of a* `R` *package.*

Reply: We have opted to submit to *PLOS ONE* because the manuscript not only introduces the **nhppp** `R` package, but also includes a review of some pertinent theory and a computational accuracy and cost study. This appears concordant with the Journal's scope and aims.

Acceptance and rejection decisions rest with the Editor. As observed by Reviewer 6, *PLOS ONE* has published analogous papers in the past. As of today, the Journal has published at least 86 papers that ostensibly introduce `R` packages.[1]

E. Reviewer 5 comments (R5)

R5.1: *This manuscript presents the* **nhppp** *package for simulating events from one-dimensional non-homogeneous Poisson point processes (NHPPPs) in* `R`*. Related work has already*

[1] Based on the PubMed query `PLOS ONE[so] AND "R package"[ti]` on July 15, 2024.

been published as a preprint. While the manuscript is comprehensive and detailed, it currently resembles a user manual for the toolbox. Before considering acceptance, I recommend that the authors supplement the conclusion with quantitative results, particularly highlighting the advantages of their package over existing toolboxes, such as improvements in efficiency and accuracy, among other metrics.

Reply: Please clarify. Extensive quantitative analyses and comparisons with other `R` packages are already presented in Sections 6 and 7 of the manuscript and in Figures 2 through 7 and Tables 3 through 8. These sections include detailed comparisons with all `R` packages that include functionality to simulate from NHPPPs and reveal that some of the existing packages simulate only approximately.

F. Reviewer 6 comments (R6)

R6.1: *This research is written and formatted in a respectable academic style comparable to studies published in the* `R` Journal. *While I recommend that authors try to publish it in the* `R` Journal*, because it is the best place for this type of research,* PLOS ONE *also accepts these types of studies. Therefore, I recommend accepting publication in* PLOS ONE *after reviewing and ensuring that it conforms to the journal's requirements.*

Reply: Thank you. We decided to submit this paper to *PLOS ONE* based on the Journal's description of its scope. The paper not only introduces a package, but does some review of theory, describes algorithms and intuition for them, includes a numerical accuracy and computational cost study, and does qualitative and quantitative comparisons with other packages. *PLOS ONE* has published papers introducing `R` packages in the past. The Journal has published at least 86 papers that ostensibly introduce `R` packages (PubMed query `PLOS ONE[so] AND "R package"[ti]` on July 15, 2024).

LaTeX Source File (TEX file)

Click here to access/download
LaTeX Source File (TEX file)
1file_plos_one_paper_R2.tex